Published in final edited form as:
J Med Chem. 2012 June 28; 55(12): 5965–5981. doi:10.1021/jm3006806.

Identification, Synthesis, and Biological Evaluation of the Metabolites of 3-Amino-6-(3'-aminopropyl)-5*H*-indeno[1,2-*c*]isoquinoline-5,11-(6*H*)dione (AM6-36), a Promising Rexinoid Lead Compound for the Development of Cancer Chemotherapeutic and Chemopreventive Agents

Lian Chen[‡,#], **Martin Conda-Sheridan**[†,#], **P. V. Narasimha Reddy**[†], **Andrew Morrell**[†], **Eun-Jung Park**[§], **Tamara P. Kondratyuk**[§], **John M. Pezzuto**[§], **Richard B. van Breemen**[‡,*], and **Mark Cushman**[†,*]

[†]Department of Medicinal Chemistry and Molecular Pharmacology, College of Pharmacy, and the Purdue Center for Cancer Research, Purdue University, West Lafayette, Indiana, 47907

[‡]Department of Medicinal Chemistry and Pharmacognosy, College of Pharmacy, The University of Illinois at Chicago, Chicago, Illinois 60612

[#]College of Pharmacy, University of Hawaii at Hilo, Hilo, Hawaii 96720

Abstract

Activation of the retinoid X receptor (RXR), which is involved in cell proliferation, differentiation and apoptosis, is a strategy for cancer chemotherapy and chemoprevention, and 3-amino-6-(3'-aminopropyl)-5*H*-indeno[1,2-*c*]isoquinoline-5,11-(6*H*)dione (AM6-36) (**3**) is among the few RXR ligands known. The presently reported studies of **3** include its binding to human plasma proteins, metabolic stability using human liver microsomes, metabolism by human liver microsomes and hepatocytes, and in vivo disposition in rat serum, liver and mammary tissue. Compound **3** was 75% bound to human plasma proteins, and its metabolic stability was much greater than propranolol. One phase I metabolite was formed by human liver microsomes, 7 phase I and II metabolites were formed by human hepatocytes, and 5 metabolites were detected in rat serum and liver after oral administration. The putative metabolites predicted using LC-MS-MS were synthesized to confirm their structures and to provide sufficient material for investigation of induction of RXRE transcriptional activity and inhibition of NFκB.

Introduction

The control of gene expression offers a powerful strategy for the prevention and treatment of disease. Human gene expression is regulated by 48 nuclear receptors, approximately one-third of which require heterodimerization with one of the ligand-activated retinoid X receptors (RXR subtypes α, β, or γ) to bind to DNA and function efficiently.[1, 2] This situation has led to RXRs being dubbed the "master partners".[3] Well-known heterodimerization partners of RXRs include the liver X receptor (LXR), the retinoic acid

[*]To whom correspondence should be addressed. Richard B. van Breemen: Tel: 312-996-9353. Fax: 312-996-7107. breemen@uic.edu. Mark Cushman: Tel: 765-494-1465. Fax 765-494-6790. cushman@purdue.edu.
[#]These authors contributed equally.

Supporting Information Available: General materials and methods for the metabolism studies and biological assays, as well as detailed experimental procedures for the syntheses of compounds **25–30** and **32–34**. This material is available free of charge via the Internet at http://pubs.acs.org.

receptor (RAR), and the vitamin D receptor (VDR).[4, 5] The RXRs also have the ability to form homodimers that possess a ligand-binding and a DNA-binding domain. The ligand-free RXR homodimers bind to DNA response elements (RXRE) and recruit corepressor-protein complexes. Upon ligand binding, the RXR homodimers undergo conformational changes that lead to dissociation of corepressor-proteins and binding of co-activator proteins, triggering transcription. This up-regulates, for example, the production of cyclin-dependent kinase inhibitor ($p21^{WAF1/CIP1}$).

Several reports have suggested that $p21^{WAF1/CIP1}$ up-regulation causes apoptosis of cancer cells.[6] Consequently, compounds that bind to an RXR and activate the RXRE may function as chemopreventive agents. This effect is observed when an RXR is activated by one of its ligands, 9-*cis*-retinoic acid (9cRA) (**1**). Various reports have documented the chemopreventive effects of 9cRA by itself or when combined with other substances.[7–10] However, therapies based on 9cRA or other retinoids are compromised by a variety of side effects, including headaches, alopecia, hypothyroidism, skin lesions, teratogenicity, and mucocutaneous toxicity.[11–17] RXR-selective ligands, known as rexinoids, have the potential to function as chemotherapeutic or chemopreventive agents[3, 18–20] without the serious side effects associated with retinoids. Although thousands of synthetic ligands are known for the retinoic acid receptors, a limited number of synthetic ligands have been discovered for the RXRs, and these rexinoids include AGN194204, CD3254, LG100268, LGD1069, and SR11237.[21] One rexinoid, bexarotene (**2**), has been launched for treatment of cutaneous T-cell lymphoma and is in advanced clinical trials for treatment of a wide variety of other types of cancer.[18, 20, 22]

The indenoisoquinoline 3-amino-6-(3'-aminopropyl)-5,6-dihydro-5,11-dioxo-11*H*-indeno[1,2-*c*]isoquinoline (AM6-36,[23] **3**) was synthesized in our laboratory and found through screening to bind to RXRα and induce apoptosis in MCF-7 breast cancer cells.[23] Since these data suggest that **3** is a promising lead compound for the treatment or prevention of breast cancer, drug development studies were carried out that included evaluation of metabolic stability, intestinal permeability, metabolic transformation by human liver microsomes and human hepatocytes, binding to human plasma proteins, and preliminary disposition studies in rats. The metabolism studies of lead compounds such as indenoisoquinoline **3** provide information regarding metabolic stability,[24, 25] the potential of forming potentially toxic metabolites,[26] and the possibility of metabolic transformation to more active (or inactive) products.[27] This report documents the identification, synthesis, and biological investigation of the metabolites of the indenoisoquinoline **3** (Figure 1).

Results

Metabolism

The positive ion electrospray LC-MS analysis of the metabolite mixture after incubation of **3** with human liver microsomes is shown in Figure 2. Major metabolite **4** (retention time 7.1 min) was detected as a protonated molecule of *m/z* 322.1554 which is within −0.2 ppm of the elemental composition $C_{19}H_{20}N_3O_2$. This formula indicates that **4** is a reduction product of **3** ($C_{19}H_{18}N_3O_2$) formed by the addition of 2 hydrogen atoms. The formation of **4** required both liver microsomes and NADPH, since omission of either produced no detectable metabolites of **3** (Figure 2). Possible chemical structures that are consistent with these data would include reduction of the ketone to an alcohol or reduction of a carbon-carbon double bond. The positive ion electrospray product ion tandem mass spectra of **3** and **4** were obtained and are shown in Figures 3A and 3B. The tandem mass spectrum of **4** (Figure 3) contained an abundant fragment ion of *m/z* 287.1107 ($C_{19}H_{15}NO$, −2.7 ppm) corresponding to the loss of ammonia and a molecule of water. Not observed in the tandem

mass spectrum of **3** (Figure 3), loss of water from **4** suggested that it was formed by reduction of the ketone of **3** to an alcohol. The corresponding alcohol was synthesized and found to co-elute with **4** during LC-MS/MS and to produce an identical tandem mass spectrum (data not shown). Therefore, **4** was identified as 3-amino-6-(3-aminopropyl)-11-hydroxy-6,11-dihydro-5*H*-indeno[1,2-*c*]isoquinolin-5-one (see structure in Figure 1).

There were 7 metabolites formed during incubation of **3** with human hepatocytes (Figure 4), and one was identical to the liver microsomal metabolite **4**. The most abundant of the hepatocyte metabolites, **5**, eluted at 27.8 min during LC-MS analysis (Figure 4) and formed a protonated molecule of *m/z* 362.1501. Accurate mass measurement of **5** indicated an elemental composition of $C_{21}H_{20}N_3O_3$ (ΔM −1.1 ppm) which corresponded to mono-acetylation of **3**. The product ion of *m/z* 345.1234 in the positive ion tandem mass spectrum (Figure 3) was formed by loss of an amino group, and this and the product ion of *m/z* 317 indicated that the acetyl group was not present on the aminopropyl side chain. Therefore, the acetyl group must be located on the aniline group (Figure 3). This proposed structure of **5** was then confirmed as *N*-(6-(3-aminopropyl)-5,11-dioxo-6,11-dihydro-5*H*-indeno[1,2-c]isoquinolin-3-yl)acetamide by LC-MS/MS comparison with a synthetic standard.

Another abundant metabolite of **3** formed by human liver microsomes, **7**, was detected during LC-MS at a retention time of 39.6 min (Figure 4). The protonated molecule of **7** was measured as *m/z* 321.1247, which corresponded to an elemental composition of $C_{19}H_{17}N_2O_3$ (ΔM 2.5 ppm). Therefore, **7** was formed by the conversion of an amino group to an alcohol. Based on the observation of fragment ions of *m/z* 303 and *m/z* 275 in the product ion tandem mass spectrum, which localized the alcohol to the propyl side chain (Figure 5), the putative metabolite was synthesized for comparison using LC-MS/MS, and **7** was identified as 6-(3-hydroxypropyl)-3-amino-5*H*-indeno[1,2-*c*]isoquinoline-5,11(6*H*)-dione (Figure 1).

To determine if monoamine oxidases were responsible for the formation of **7**, human liver microsomes were preincubated with the monoamine oxidase A and B inhibitors clorgiline and pargyline immediately before incubation with **3**. Since these inhibitors did not alter the formation of **7** from **3** (data not shown), monoamine oxidases were not responsible for this metabolic transformation. These results indicate that **3** will not interfere with monoamine oxidase metabolism.

Eluting at 26.9 min (Figure 4), the protonated molecule of **8** was detected at *m/z* 323.1383 and corresponded to a theoretical formula of $C_{19}H_{19}N_2O_3$ (ΔM −4.0 ppm). The fragment ions of *m/z* 305 ($[MH\text{-}H_2O]^+$), *m/z* 287 ($[MH\text{-}2H_2O]^+$), 277, and *m/z* 264 in the product ion tandem mass spectrum of **8** (Figure 5) indicated the presence of two alcohol groups with one located at the terminus of the propyl side chain. These data are consistent with reduction of the ketone to an alcohol and conversion of the amino propyl group to a propyl alcohol group. After synthesis of this proposed compound and comparison with the metabolite using LC-MS/MS, **8** was identified as 3-amino-11-hydroxy-6-(3-hydroxypropyl)-6,11-dihydro-5*H*-indeno[1,2-*c*] isoquinolin-5-one (Figure 1). Metabolite **6** eluted at a retention time of 22.1 min (Figure 4) and was detected as a protonated molecule of *m/z* 364.1662. Accurate mass measurement indicated an elemental composition of $C_{21}H_{22}N_3O_3$ (ΔM 0.3 ppm), which likely corresponded to the addition of an acetyl group to **4** since several fragment ions of **7** differed from **4** by 42 u (a ketene, C_2H_2O, which is a characteristic neutral loss of acetyl groups) including *m/z* 233, 275, 290, 319, 329, and 347 (Figure 5). Since $[MH\text{-}NH_3]^+$ was observed as the base peak of *m/z* 347 (Figure 5), acetylation did not occur on the aminopropyl group. Therefore, a derivative of **4** was synthesized containing an acetyl group on the aniline group (Figure 1). Based on identical tandem mass spectra and co-

elution during LC-MS/MS, **6** was identified as *N*-(6-(3-aminopropyl)-11-hydroxy-5-oxo-6,11-dihydro-5*H*-indeno[1,2-*c*]isoquinolin-3-yl)acetamide.

A minor metabolite of **3**, **9** eluted at a retention time of 42.3 min (Figure 4). Using positive ion electrospray with accurate mass measurement, protonated **9** was measured at *m/z* 363.1346 which was within 0.3 ppm of the elemental composition $C_{21}H_{19}N_2O_4$. This elemental composition suggested acetylation and conversion of an amino group to an alcohol. Since the tandem mass spectrum of **9** (Figure 6) was similar to that of **5** (Figure 3), **9** was likely to be acetylated like **5** but differ by conversion of the aminopropyl group to an alcohol. The predicted metabolite was synthesized and shown to co-elute with **9** during LC-MS/MS and to produce an identical tandem mass spectrum. Therefore, the structure of **9** was determined to be *N*-[6-(3-hydroxypropyl)-5,11-dioxo-6,11-dihydro-5*H*-indeno[1,2-*c*]isoquinolin-3-yl]acetamide (Figure 1).

Metabolite **10** eluted at 20.2 min (Figure 3), and formed a protonated molecule of *m/z* 496.1734. Accurate mass measurement indicated an elemental composition of $C_{25}H_{26}N_3O_8$ (ΔM 2.8 ppm). Since the mass was 176 u higher than **3**, **10** was probably a monoglucuronide. After treatment with β-glucuronidase and re-analysis using LC-MS (data not shown), the peak of **10** disappeared and the peak corresponding to **3** increased, which confirmed the identification of **10** as a glucuronic acid conjugate of **3**. The ion of *m/z* 479.1307 in the product ion mass spectrum of **10** (Figure 6) represented loss of an amino group from the protonated molecule, suggesting that the aminopropyl group was not conjugated with glucuronic acid. Although no authentic standard was synthesized for confirmation, **10** was probably a monoglucuronide of **3** conjugated on the nitrogen substituent of the A-ring (Figure 1).

Determination of Metabolic Stability

The concentration of **3** decreased during incubation for 60 min with human liver microsomes (Figure 7). The elimination rate constant of **3** was 0.0053, and the in vitro half-life was 130 min. Based on these data, the hepatic intrinsic clearance of **3** was determined to be 5.33 mL/min/kg. Under identical conditions, the reference substrate propranolol, which has medium-low metabolic stability,[28] showed an elimination rate constant of 18.3 mL/min/kg and a half-life of 38 min.

Test for Electrophilic Metabolites of 3

During the investigation of the metabolism of **3** by human liver microsomes, a set of experiments was carried out containing the biological nucleophile glutathione to trap any electrophilic metabolites that might form. Analysis of the metabolite mixture using LC-MS/MS showed no evidence of glutathione conjugates (data not shown). Therefore, human liver microsomal metabolism of **3** does not appear to generate any electrophilic intermediates that can be trapped as glutathione conjugates.

Human Plasma Protein Binding of 3

Equilibrium dialysis and LC-MS/MS were used to investigate the binding of **3** to human plasma proteins. Compound **3** was found to be 75% bound to plasma proteins. For comparison, ketoconazole, which was used as a high protein binding control, was 95% bound to plasma proteins under identical conditions, and only 7% of the low protein binding control, atenolol, was found to be bound to plasma proteins.

In Vivo Metabolism of 3

After administration of **3** to rats by gavage, serum, liver and mammary tissues were obtained for analysis using high-resolution LC-MS and LC-MS/MS. As reported previously,[23] **3** was measured in serum, liver, and mammary gland at 0.8 μg/mL, 4.3 μg/g and 0.3 μg/g, respectively. The acetylated **3** metabolite, **5**, which was the most abundant phase II metabolite in vitro, was also the most abundant metabolite observed in vivo and was detected in serum and rat liver but not in mammary tissue. In addition to **5**, metabolites **4**, **7**, **8**, and **9** were detected in rat liver but not in serum or mammary tissue. The identities of these metabolites in rat serum and liver were confirmed by comparison of the tandem mass spectra and HPLC retention times of the metabolites with synthetic standards.

Discussion of Metabolism

During in vitro evaluation, **3** showed only moderate binding to serum proteins (75%) and should not produce drug-drug interactions due to displacement of highly bound drugs from serum proteins. The metabolic half-life of **3** (130 min) was longer than propranolol (38 min), and its hepatic intrinsic clearance (5.33 mL/min/kg) was considerably larger. Note that the measured hepatic intrinsic clearance of propranolol, 18.3 mL/min/kg, was similar to the literature value of 13 mL/min/kg.[29] Therefore, **3** is predicted to have low first-pass hepatic metabolism.

During incubation with human liver microsomes and NADPH, one metabolite was observed, **4**, which was formed by reduction of the ketone group on the C-ring to an alcohol (Figure 1). Incubation with human hepatocytes produced 7 metabolites, 4 of these were formed in approximately equal abundance (**4**, **5**, **7**, and **8**) and 3 were minor metabolites (**10**, **6** and **9**) (Figure 4). Three of these hepatocyte metabolites, **4**, **6** and **8**, contained an alcohol on the C-ring due to reduction of the ketone. The abundant metabolite **5** was formed by acetylation of the amino group on the aromatic A-ring (Figure 1) instead of the amino group on the propyl side chain, probably due to pKa differences, which would cause the aliphatic amine to be protonated at physiological pH and therefore less susceptible to acetylation. Compounds **6** and **9**, which were observed in low abundance, were probably formed from metabolite **5** by reduction of the ketone or conversion of the aliphatic amine to an alcohol, respectively. Alternatively, **9** could have been formed by acetylation of metabolite **7**, which was generated from **3** by conversion of the aliphatic amine to an alcohol. Metabolite **8** was the only diol metabolite which might have been formed by reduction of the ketone of metabolite **7** or oxidation of the aliphatic amine of metabolite **4** followed by reduction of the intermediate aldehyde. Observed only as a minor metabolite, **10** was the only glucuronide formed from **3** by human hepatocytes.

Among the 7 metabolites of **3** observed in vitro, all except **6** and **10** were observed in vivo using rats. Among the metabolites of **3** detected in vivo, **4** was the most abundant. These findings are consistent with the in vitro studies for the following three reasons: 1) **4** was a major metabolite of **3** during incubations with human hepatocytes; 2) **4** was the only metabolite formed by human liver microsomes; and 3) **6** and **10** were only minor metabolites formed by human hepatocytes. Ketone reduction has also been reported to be a major metabolic reaction of the structurally related cytostatic agent oracine, both in vitro and in vivo.[30]

Since metabolites of **3** might also have therapeutic activities, studies are in progress to investigate this possibility. The metabolic activation experiments using glutathione as a trapping agent showed no evidence of the formation of electrophilic metabolites, which might be a source of toxicity.[31]

Chemistry

With the exception of the glucuronide, all of the compounds having the structures assigned to the metabolites were synthesized in order to obtain authentic reference standards that could be used to confirm the identities of the actual metabolites. The syntheses of the metabolites was also carried out to provide enough material for investigation of their biological activities.

The synthesis of the indenoisoquinoline **3** has been previously reported.[23] The first compound that was prepared was metabolite **4**. This molecule was synthesized by reduction of the carbonyl ketone of **3** with sodium borohydride in methanol (Scheme 1). Metabolite **4** proved to be rather unstable and slowly oxidized back to **3** in the presence of air and moisture or while in DMSO solution.

Because of the higher nucleophilicity of the aliphatic aminopropyl nitrogen of **3** compared with its aniline nitrogen, the acetylated metabolite **5** could not be prepared by direct treatment with an acylating agent. In order to circumvent this problem, indenoisoquinoline **11** was prepared[32] and its nitro group was reduced under standard catalytic conditions to yield **12** (Scheme 2).[33] Treatment of this compound with acetyl chloride afforded indenoisoquinoline **13**. The chloride of this intermediate was then replaced by an azide group to provide compound **14**. The azide functionality was converted into an amino group in order to obtain the desired metabolite **5** in 10% overall yield from the starting material **11**. Also, some **3** was recovered due to removal of the acetyl moiety. Reduction of **5**, as previously done with **3**, afforded metabolite **6**.

An alternative synthesis of metabolite **5** was devised in order to improve the overall yield (Scheme 3). Indenoisoquinoline **15** was prepared as previously reported[32] and protected with di-*tert*-butyl dicarbonate to give **16**.[34] Subsequent reduction of the nitro group to produce **17**, acetylation of the aniline to yield **18**, and removal of the protective group under acidic conditions afforded the acetylated metabolite **5** in 49% overall yield from compound **15**.

As stated earlier, the aminopropyl nitrogen is the most nucleophilic of the nitrogens in compound **3**. In order to confirm the correct location of the acetyl moiety in the proposed metabolite structure **5** it was necessary to prepare the alternative compound **20**. The amino group of the starting material **15** was acetylated to give **19**, and catalytic hydrogenation of this compound afforded **20** (Scheme 4).

In order to prepare metabolites **7** and **8** (Scheme 5), isochrominone **21**[35] was reacted with 3-hydroxy-1-propylamine (**22**) to give **23**, which was converted to the proposed metabolite **7** by reducing the nitro substituent with palladium on charcoal in a hydrogen atmosphere. Further reduction with sodium borohydride afforded metabolite **8**.

Metabolite **9** of this series was prepared in one pot from compound **24** (Scheme 6). Briefly, the nitro group of precursor **24**[36] was reduced with iron and ammonium chloride. The solution was neutralized with sodium hydroxide,[37] the intermediate acetylated,[38] and the mixture treated again with sodium hydroxide to afford the desired metabolite **9**.

During the course of this study, several potential metabolites of compound **3** were prepared to determine if they would match any unidentified actual metabolites. Treatment of **17** with formaldehyde under reductive amination conditions[39] produced the monomethylated compound **25** and the dimethylated analogue **26** (Scheme 7). Reduction of the ketone of **25** and removal of the protecting group afforded **29**. Given the preliminary biological data

indicating that the ketone was essential for RXRE agonist activity, compound **12** was converted to **30** (Scheme 8).

A final set of analogues was prepared by reacting isochrominone **21** with compound **31** to afford **32** (Scheme 9). Dissolving metal reduction to obtain **33**, followed by treatment with sodium borohydride, produced compound **34**. None of the compounds prepared in Schemes 7–9 matched any of the substances detected in the metabolism studies. They were, however, subjected to biological analyses along with the metabolites, and several of them had significant activity (Table 1).

Biological Evaluations

RXRE

As stated in the introduction, the induction of RXRE transcriptional activity is a valid chemopreventive strategy. The metabolites of **3** and the intermediates and analogues produced in their synthesis were tested against this target. The main objective of this part of the study was to investigate the activities of the metabolites, but in the process some limited insight into the SAR of the indenoisoquinoline rexinoids was also produced.

The biological evaluation indicates that one metabolite (**5**) and three analogues (**20**, **30**, and **33**) have RXRE induction activity. Compounds **5** and **20** presented maximum induction ratios (IR) of 3.55±0.53 and 3.52±0.33, respectively (Table 1). These values are approximately half the activity of the parent compound, **3**, which has a maximum IR of 7.67±0.37. The other two compounds, **30** and **33**, have maximum IR values of 6.09±0.51 and 8.97±0.71, which are in the same range as **3**. Compound **33** had a higher EC_{50} value than **3**, 9.96±2.26 vs. 3.37±0.51 μM. It also had a higher maximum IR and was less cytotoxic than **3**. Moreover, compound **33** can achieve an IR similar to the clinically used bexarotene (**2**) at approximately one third molar concentration (8.97±0.71 at 12.5 μM vs 8.85±3.89 at 40 μM, respectively).[23] These facts make compound **33** a promising lead for further studies. Figure 8 shows the results for the active compounds at different concentrations.

The data also revealed some insights into the critical structural features necessary for maintaining RXR agonist activity. For example, the ketone is important for activity. When this group was converted to an alcohol the compounds became inactive (**3** vs. **4** or **5** vs. **6**). In general, a 3-amino propyl or substituted 3-aminopropyl side chain is critical for activity. When the amine is exchanged for an alcohol, halide, or azide, the activity also drops (**3** vs. **7**, **3** vs. or **12**, or **5** vs. **14**). Acylation of the aminopropyl side chain is also detrimental for RXR agonist activity (**3** vs. **17** or **20**). The substitution of the 3-amino group with a 3-nitro group increases cytotoxicity and abolishes the activity (**3** vs. **15** and **33** vs. **34**). If both of the hydrogens on the aniline nitrogen are replaced by methyl groups, the RXR agonist activity also drops due to cytotoxicity (**3** vs. **28**). When an acetyl group is attached to the aniline or aliphatic nitrogens of the active indenoisoquinoline as the only modification, the compounds maintain activity but the IR drops (**3** vs. **5** or **20**).

A comparison between the activity mediated by compound **3** and a known rexinoid standard, bexarotene, is illustrated in Figure 9. Following an incubation period of 2 h, treatment with compound **3** or bexarotene moderately induced RXRE transcriptional activity. However, after 4–6 h of incubation, treatment with compound **3** or bexarotene enhanced transcriptional activity by a maximum of 5- and 10-fold, respectively. While bexarotene exerted higher induction of RXRE transcriptional activity at each treatment concentration at these early time points, significantly greater activity was exerted by compound **3** after a 24 h incubation period (~160-fold induction at a concentration of 5 μM).

RXR homodimer-driven transcriptional activation via interaction with RXRE *cis*-acting element in the promoter region results in the expression of firefly luciferase gene, leading to increased luminescence by enzymatic activity. However, since RXR is known to induce apoptosis,[40] a reduction in apparent firefly luciferase activity may be observed. In this case, however, the absolute activity induced by compound **3** (40.5 ± 5.4-fold) was approximately 2-fold higher than induced by bexarotene (22.4 ± 3.1-fold) under these incubation conditions. Moreover, as shown in Figure 9, when the data were normalized on the basis of *Renilla* luciferase activity (which correlates with cell survival),[41] the induction ratio observed with compound **3** exceeded 100-fold.

NFKB

Nuclear factor kappa beta (NFKB) is a transcription factor that regulates several biological responses such as cell survival, proliferation and expression of cytokines, cyclooxygenase 2 (COX-2) and inducible nitric oxide synthase (iNOS).[42–45] The aberrant activation or overexpression of this transcription factor is linked to several cancers.[42, 43, 46] Inhibition of NFκB blocks tumor growth and cancer cellular proliferation, induces apoptosis of cancer cells and modulates COX-2 and iNOS expression, making this an interesting chemopreventive target.[46–50]

RXR belongs to a family of ligand-activated transcription factors capable of affecting multiple biological pathways. In relation to NFκB, RXR complexes may regulate activity by sequestering co-activators and through cross-coupling and inhibition.[51] In mouse macrophages, retinoids inhibit LPS-stimulated production of IL-12 through direct interaction of retinoid receptors with NFκB.[52] This inhibitory complex appears to be involved in reducing NFκB binding with DNA as well as competitive recruitment of transcription integrators between NFκB and RXR. In addition, rexinoids have the potential of being used in a synergistic fashion with NFκB inhibitors for the control inflammatory processes as well as cancer,[53] and some compounds with structures similar to the indenoisoquinolines have shown NFκB inhibitory activity.[54, 55] Based on these considerations, the compounds produced during the course of this investigation were evaluated for potential to inhibit NFκB activity.

As shown in Table 1, compound **3** showed moderate NFκB inhibitory activity with an IC_{50} of 26.3±3.0 μM. However, compounds **27**, **29** and **34** (not active as RXR agonists), inhibited NFκB activity at sub-μM concentrations, and others were active in the range of 2–50 μM. Based on these data, structural features relevant to NFκB inhibition can be considered. For example, the amino group on the propyl side chain confers better activity that its alcohol analogues (**3** vs. **7** and **15** vs. **23**). Compounds lacking hydrogen bond donors on the side chain are inactive or have low activity (see **12**, **14**, and **24**). In compounds with an aminopropyl side chain, acetylation of the aniline nitrogen abolishes the NFκB inhibitory activity (e.g. **3** vs. **5** and **4** vs. **6**). However, acetylation of the aniline nitrogen in the hydroxypropyl derivative **7** does not decrease the activity (compare **7** with **9**). Additionally, the nitro-substituted indenoisoquinolines are generally more active than their aniline counterparts (**3** vs. **15**, **7** vs. **23**, and **32** vs. **33**), but compounds **19** and **20** are an exception. In some cases, reduction of the ketone to an alcohol resulted in higher inhibitory activities (**33** vs. **34** and **25** vs. **27**), but in the case of **3** vs. **4**, the ketone **3** was more active. *N*α-Tosyl-L-phenylalanine chloromethyl ketone (TPCK) and BAY-11 were used as a positive controls and exerted inhibitory activity with IC_{50} values of 5.1±1.6 and 2.01±0.37 μM, respectively.

Conclusions

The metabolism of the indenoisoquinoline **3**, which is an agonist of RXR under investigation as a potential chemotherapeutic and chemopreventive agent, was investigated using human hepatocytes, human liver microsomes and rats. Compound **3** formed 7 phase I and phase II metabolites. Structures for all 7 of the metabolites **4**–**10** were proposed based on high resolution accurate mass tandem mass spectrometry, and 6 of these metabolites were identified by comparison with synthetic standards. These preliminary metabolism studies suggest that **3** will not form reactive, potentially toxic metabolites. Compound **3** showed moderate serum protein binding, moderate metabolic stability, and low first-pass liver metabolism is predicted. The structures of six human metabolites (**4–9**) of the RXRE inducer **3** were suggested by MSMS analysis.

The syntheses of the metabolites and several analogues have been achieved in a simple and efficient fashion. The metabolic products arise from reduction of the carbonyl ketone, acetylation of the aniline nitrogen, methylation of the aliphatic nitrogen or a combination of these events. All of the metabolites were inactive as inducers of RXRE transcriptional activity except for the acetylated compound **5**, which was moderately active at high concentrations. Two indenoisoquinoline compounds, **30** and **33**, showed similar potencies as the lead compound **3**. This is noteworthy because most of the RXRE inducers found in the literature possess an acidic moiety. Therefore, the indenoisoquinolines are a novel class of rexinoids.[23] Finally, several potenit indenoisoquinoline inhibitors of NFκB have been found, including compounds **29** and **34**, and this is the first report of activity of this class of compounds against this target. That being said, all of the metabolites were inactive as inhibitors of NFκB with the exception of **8**, which inhibited activity as high concentrations (Table 1). In sum, indenoisoquinolines **3** and structurally related compounds constitute a novel class of rexinoids and inhibitors of NFκB. Studies are underway to further optimize the activities of these compounds as chemopreventive and chemotherapeutic agents.

Experimental Section

Metabolism of 3 by Human Liver Microsomes

Compound **3** (1 μM) was incubated at 37 °C with pooled human liver microsomes (10 donors, mixed gender) containing 1 mg/mL of microsomal protein and 50 mM phosphate buffer at pH 7.4 in a total volume of 200 μL. After a 10 min preincubation, 1 mM NADPH was added to initiate reaction, and the mixture was incubated for an additional 60 min. The reaction was stopped by chilling the mixture on ice and by addition of 20 μL of ice-cold acetonitrile/water/formic acid (86:10:4, v/v/v) to precipitate proteins. Samples were centrifuged, supernatants were removed, evaporated to dryness under nitrogen, and the residues were dissolved in the mobile phase prior to analysis using liquid chromatography-mass spectrometry (LC-MS) and LC-tandem mass spectrometry (LC-MS/MS). Control incubations were identical except for the elimination of microsomal protein or NADPH. To determine if monamine oxidases participated in the formation of metabolites of **3**, incubations with human liver microsomes was repeated as described above except that 15 min preincubation was carried out with 10 μM clorgiline or 10 μM pargyline, which are inhibitors of monoamine oxidases A and B, respectively.

Metabolism of 3 by Human Hepatocytes

Cryopreserved hepatocytes were thawed according to the supplier's instructions, and approximately 1×10^6 cells in a 1 mL suspension were incubated with 50 μM **3** per well of a 6-well plate. Control experiments were identical except for the use of heat-inactivated hepatocytes. The plate was incubated for 4 h at 37 °C with 5% CO_2 and 90% relative

humidity. Incubations were terminated by the addition of 3 mL of ice-cold acetonitrile. The cell suspensions were centrifuged, and aliquots of the supernatants were analyzed using LC-MS and LC-MS/MS.

A 500 μL aliquot of the hepatocyte preparation was evaporated to dryness and reconstituted in 500 μL sodium acetate buffer (100 mM, pH 5.0) containing β-glucuronidase (800 units). Enzymatic deconjugation was carried out at 37 °C for 6 h and then terminated by the addition of 3 volumes of ice-cold acetonitrile. After centrifugation, aliquots of the supernatants were analyzed using high resolution LC-MS/MS. Samples not treated with β-glucuronidase were used as controls.

Determination of Metabolic Stability

To investigate metabolic stability, **3** (1 μM) or propranolol (reference compound with medium metabolic stability[28]) was incubated with human liver microsomes (1 mg protein/mL) as described above except that the total incubation volume was 500 μL. Aliquots (50 μL each) were removed at 0, 5, 10, 20, 30, 40, 50, and 60 min, and mixed with 10 μL ice-cold acetonitrile/water/formic acid (90:10:4, v/v/v) containing ketoconazole (2.5 μM) as an internal standard. After centrifugation to remove the precipitated protein, the concentration of **3** or propranolol was determined in each supernatant using LC-MS/MS.

The hepatic intrinsic clearances of **3** and propranolol were determined based on the rates of substrate disappearance during incubation with human liver microsomes. The slope of the linear regression curve ($-k_e$) from log percentage remaining of each compound versus incubation time was used to compute half-life using the following equation: $t_{1/2} = -0.693/k_e$. Values of 50 mg protein/g liver and 20 g of human liver per kilogram body weight were used for W_{liver} and W_{body}, respectively.[56] Then, hepatic intrinsic clearance (CL_{int}, mL/min/kg) was calculated by using the following equation:

$$CL_{\text{int}} = \frac{0.693}{t_{1/2} \cdot C_{protein}} \cdot \frac{G_{micrs}}{W_{liver}} \cdot \frac{W_{liver}}{W_{body}} = \frac{1000 \times 0.693}{t_{1/2} \cdot C_{protein}}$$

Testing for Formation of Electrophilic Metabolites

Compound **3** (10 μM), human liver microsomes (1 mg protein/mL), glutathione (10 mM), and NADPH (1 mM) were incubated in 400 μL of 50 mM phosphate buffer (pH 7.4). A negative control was prepared containing no microsomes. The samples were incubated at 37 °C for 60 min and centrifuged. Aliquots of the supernatants were analyzed for glutathione conjugates using LC-MS/MS as described previously.[31]

Human Plasma Protein Binding of 3

Human plasma, spiked with 10 μM **3**, was added to the sample chamber of a rapid equilibrium dialysis kit, and 350 mL of phosphate-buffered saline (containing 100 mM sodium phosphate and 150 mM sodium chloride, pH 7.4) was added to the buffer chamber. The plate was sealed and incubated at 37 °C on an orbital shaker at 100 rpm for 5 h. Note that 5 h incubation time was used since preliminary experiments indicated that binding of **3** to human plasma proteins reached equilibrium by approximately 4.5 h. Aliquots (50 μL) were removed from the sample and buffer chambers and mixed with an equal volume of buffer or blank plasma, respectively. To each sample, 300 μL of ice-cold acetonitrile was added, and the matrix-matched samples were vortex mixed and incubated for 30 min on ice. After centrifugation at 13,000×*g* for 15 min, the supernatants were removed, evaporated to dryness and then reconstituted in acetonitrile/water containing 0.1% formic acid (30:70, v/v) and 0.5 μM of caffeine (internal standard) prior to quantitative analysis using LC-MS/MS.

The plasma protein binding of ketoconazole and atenolol, high and low plasma binding reference compounds, respectively, were also determined. The percentage of each compound bound to plasma protein was calculated as follows:

% Free = (Concentration in buffer chamber/Concentration in plasma chamber) × 100%

% Bound = 100% - % Free

Detection of Metabolites of 3 In Vivo

Female Sprague-Dawley rats were received at 4-weeks-of-age from Harlan (Indianapolis, IN) and placed on Teklad diet. At 77 days-of-age, the rats were administered **3** by gavage (40 mg/kg, 0.5 mL ethanol/polyethylene glycol 400, 10:90, v/v) daily for 3 days. Blood samples were collected (jugular vein) 3 h after the first treatment. Three hours after the third and final treatment, the animals were sacrificed, and blood, mammary tissue and liver were collected. Serum and tissue samples were stored at −80 °C until analysis. Rat liver was homogenized in 0.05 M phosphate buffer (pH 7.4), and mammary gland tissues were homogenized in a mixture of phosphate buffer and methanol (50:50; v/v) to give homogenates containing 0.2 g tissue/mL. Proteins in the homogenized tissue and serum were precipitated with 4 volumes of ice-cold acetonitrile. After centrifugation at 13,000×*g* for 15 min, each supernatant was removed, evaporated to dryness, and reconstituted for analysis using LC-MS/MS.

LC-MS and LC-MS/MS

Analyses of **3** and its metabolites were carried out using a Waters (Milford, MA) 2690 HPLC system equipped with a Waters Xterra 2.1×100 C_{18} column. The solvent system consisted of a linear gradient from 0.1% formic acid in water to methanol as follows: 10% to 45% methanol over 35 min, 45% to 90% methanol over 10 min and isocratic 90% methanol for another 5 min. The column was equilibrated with 10% methanol for at least 10 min between analyses. The flow rate was 0.2 mL/min, and the column temperature was 33 °C. The HPLC was interfaced with a high resolution Waters Q-TOF Synapt hybrid quadrupole/time-of-flight mass spectrometer, and positive ion electrospray was used for sample ionization. For accurate mass measurements, leucine enkephalin ($[M+H]^+$ of *m/z* 556.2771) was introduced post-column as a lock mass. The mass accuracy obtained was < 5 ppm. Data were acquired from *m/z* 50–800. Tandem mass spectra were acquired at a collision energy of 25 eV using argon as the collision gas at a pressure of 2.0×10^{-5} mbar.

For quantitative analysis of **3**, internal standards and reference standards for plasma protein binding and metabolic stability studies, LC-MS/MS analyses were carried out on a Shimadzu (Kyoto, Japan) Prominence HPLC system interfaced with an Applied Biosystems (Foster City, CA) API 4000 triple quadrupole mass spectrometer. A Thermo (Bellefonte, PA) Hypersil GOLD 2.1×100 mm, 5 μm analytical column was used for chromatographic separations with a 10 min linear gradient from 10% to 90% acetonitrile in water containing 0.1% formic acid at a flow rate of 0.2 mL/min. Analytes were detected using positive ion electrospray, collision-induced dissociation and selected reaction monitoring (SRM) at unit resolution. Nitrogen was used as the collision gas at 25 eV, and the dwell time was 1000 ms/ion. During SRM, **3** was measured by recording the signal for the transition of the protonated molecule of *m/z* 320 to the most abundant fragment ion of *m/z* 303. The SRM transitions of *m/z* 531 to *m/z* 489, *m/z* 260 to *m/z* 183, *m/z* 267 to *m/z* 145, and *m/z* 195 to *m/z* 138 were monitored for ketoconazole, propranolol, atenolol, and caffeine, respectively.

RXRE-luciferase Reporter Gene Assay (RXRE Assay)

All cell lines were grown in media supplemented with penicillin G (100 units/ml), streptomycin (100 μg/mL), and heat inactivated FBS and penicillin G (100 units/mL) and

streptomycin (100 μg/mL) at 37°C in 5% CO_2 in a humidified incubator. The assay was performed as described previously by Park *et al.*[23] with a slight modification. Briefly, after the transient transfection of pRXRE (100 ng/well), phRXRα (50 ng/well), and pRL (3 ng/well) by Lipofectamine™ 2000 for 24 h, COS-1 cells were incubated with compounds or vehicle (DMSO) for additional 12 h. Cells were lysed and the RXRE transcriptional activities of compounds were determined by measuring the luciferase activities using Dual-Luciferase® Reporter Assay System. Bexarotene was used as a positive control (standard drug) for this assay. Firefly luciferase activities were normalized to *Renilla* luciferase activities, termed the relative luciferase activities, by dividing relative light unit (RLU) from firefly luciferase activities by RLU from *Renilla* luciferase activities. Then, data are presented as fold changes comparing to the value of control (fold-change of control: 1.0).

NFκB Assay

Human embryonic kidney cells 293 Panomic (Fremont, CA) were used for monitoring any changes occurring along the NFκB pathway. Stable constructed cells were seeded into sterile 96-well plate at 20 X 10^3 cells per well. Cells were maintained in Dulbecco's modified Eagle's medium (DMEM) Invitrogen Co. (Carlsbad, CA), supplemented with 10% FBS, 100 units/mL penicillin, 100 μg/mL streptomycin, 2 mM L-glutamine. After 48 h incubation, the medium was replaced and various test compouns were added to yield the indicated final concentrations. TNF-α was used as activator (Human, Recombinant, *E. coli*, Calbiochem (Gibbstown, NJ) at a concentration of 2 ng/mL (14 nM). The plate was incubated for 6 h. Spent media were discarded and the cells were washed once with PBS. Cells were lysed using 50 μL/well Reporter Lysis Buffer (Promega), by incubating for 5 min on a shaker. The luciferase assay was performed using the Luc assay system from Promega (Madison, WI).[57] The gene product, luciferase enzyme, reacts with luciferase substrate, emitting light which was detected in a luminometer (LUMIstar Galaxy BMG). NFκB data is expressed as IC_{50} values (i.e., concentration required to inhibit TNF-activated NFκB activity by 50%). *N*α-Tosyl-L-phenylalanine chloromethyl ketone (TPCK) and BAY-11 were used as a positive controls.

Chemistry General Methods

NMR spectra were obtained at 300 or 500 (^{1}H) and 75 or 125 (^{13}C) MHz in $CDCl_3$ or DMSO-*d6* using Bruker ARX300 or Bruker DX-2 500 (QNP probe or BBO probe, respectively) spectrometers unless otherwise indicated. Flash chromatography was performed with 230–400 mesh silica gel. Melting points were determined using capillary tubes with a Mel-Temp apparatus and are uncorrected. IR spectra were obtained as films on salt plates with CH_2Cl_2 as solvent or as KBr pellets, using a Perkin-Elmer 1600 series FTIR spectrometer. HPLC analyses were performed on a Waters 1525 binary HPLC pump/Waters 2487 dual λ absorbance detector system using a 5 μM C_{18} reverse phase column. All yields refer to isolated compounds. Unless otherwise stated, chemicals and solvents were of reagent grade and used as obtained from commercial sources without further purification. The purities of all of the tested compounds was >95% as determined by HPLC.

3-Amino-6-(3-aminopropyl)-11-hydroxy-6,11-dihydro-5*H*-indeno[1,2-*c*]isoquinolin-5-one (4)

3-Amino-6-(3-aminopropyl)-5*H*-indeno[1,2-*c*]isoquinoline-5,11(6*H*)-dione hydrochloride (**3**, 107 mg, 0.30 mmol) was dissolved in methanol (15 mL) and the reaction mixture was cooled to 0 °C. Sodium borohydride (1.03 g, 27.2 mmol) was added in portions and the reaction mixture was stirred for 45 min, keeping the temperature constant. The reaction mixture went from a light purple color to a yellow color and constant bubbling was observed. An aqueous solution of saturated ammonium chloride (50 mL) was added and the solution extracted with dichloromethane (5 × 20 mL). The organic extracts were dried with

sodium sulfate and the solvent removed. The obtained solid was washed with hexane-dichloromethane, 2:1. The desired compound was obtained as a dark yellow solid (73 mg, 76%): mp 194 °C (dec). IR (KBr) 3348, 3222, 3065, 2931, 2866, 1627, 1576, 1469, 1379, 1318, 1181, 1113, 833, 762 cm^{-1}; ^1H NMR (300 MHz, DMSO-d_6) δ 7.81-7.75 (m, 2 H) 7.57 (d, J = 6.9 Hz, 1 H), 7.39-7.27 (m, 3 H), 7.05 (dd, J = 6.5 Hz, J = 1.9 Hz, 1 H), 5.66-5.63 (m, 3 H), 5.43 (d, J = 8.8 Hz, 1 H), 4.49 (br t, J = 7.1 Hz, 2 H), 2.65 (br t, 2 H), 1.80 (br s, 2 H); EIMS *m/z* (rel intensity) 322 (MH^+, 100); HRESIMS *m/z* expected for $C_{19}H_{19}N_3O_2$ 322.1556 (MH^+), found 322.1558 (MH^+); HPLC purity: 98.02% (C_{18} reverse phase, MeOH-H_2O, 70:30), 96.20% (C_{18} reverse phase, MeOH, 100).

N-[6-(3-Aminopropyl)-5,11-dioxo-6,11-dihydro-5*H*-indeno[1,2-*c*]isoquinolin-3-yl]acetamide (5). Method 1

N-(6-(3-Azidopropyl)-5,11-dioxo-6,11-dihydro-5*H*-indeno[1,2-*c*]isoquinolin-3-yl)acetamide (**14**, 203 mg, 0.59 mmol) was dissolved in benzene (20 mL). Triethylphosphite (0.50 mL, 2.87 mmol) was added and the reaction mixture was heated at reflux for 12 h. The reaction mixture was cooled to room temperature and hydrochloric acid (4 mL, 1.25 M solution in methanol) was added. The reaction mixture was stirred for 20 min at room temperature and placed in the refrigerator for approximately 1 h. The precipitate was filtered and washed with dichloromethane-hexane, 1:1. The solid was then dissolved in methanol and potassium carbonate (150 mg) was added. The solution was heated until it boiled, the solvent was removed, and the compound purified by silica gel column chromatography, eluting with chloroform-methanol-triethylamine, 20:1:0.1. The title compound was obtained as a purple solid (39 mg, 18%): mp 310–312 °C. **Method 2**. *tert*-Butyl (3-(3-amino-5,11-dioxo-5*H*-indeno[1,2-*c*]isoquinolin-6(11*H*)-yl) propyl)carbamate (**17**, 65 mg, 0.15 mmol) was dissolved in tetrahydrofuran (5 mL) and the reaction mixture was cooled to 0 °C. Acetyl chloride (0.1 mL) was added and the reaction mixture stirred for 1 h keeping the temperature constant. The solvent was removed and the residue passed through a short silica gel column, eluting with chloroform-methanol, 10:1. The obtained solid **18**, without further purification, was dissolved in tetrahydrofuran (5 mL) Trifluoroacetic acid (0.1 mL) and hydrochloric acid (0.2 mL, 1.25 M solution in methanol) were added, and the reaction mixture stirred for 2 h. A solution of potassium carbonate in water (100 mg in 2 mL) was added and the reaction mixture heated at reflux for 5 min. The solution was diluted with chloroform (10 mL) and washed with water and brine (20 mL each). Purification as before gave compound **5** as a purple solid (38 mg, 70%). IR (neat) 3065, 1650, 1570, 1531, 1454, 1432, 1389, 1305, 1017, 908 cm^{-1}; ^1H NMR (300 MHz, $CDCl_3$) δ 10.34 (s, 1 H), 8.47 (s, 1 H), 8.31 (d, J = 8.7 Hz, 1 H), 7.83 (d, J = 8.7 Hz, 1 H), 7.65 (d, J = 7.4 Hz, 1 H), 7.49-7.38 (m, 3 H), 4.45 (br t, 2 H), 2.95 (t, J = 7.0 Hz, 2 H), 2.06 (br s, 5 H); ^{13}C NMR (125 MHz, DMSO-d_6) δ 190.3, 169.0, 162.8, 154.7, 138.8, 136.8, 134.5, 134.3, 131.3, 127.4, 125.9, 123.7, 123.6, 122.9, 116.7, 107.7, 41.7, 36.8, 27.5, 24.4; ESIMS *m/z* (rel intensity) 362 (MH^+, 100); HRESIMS *m/z* expected for $C_{21}H_{19}N_3O_3$ 362.1505 (MH^+), found 362.1503 (MH^+); HPLC purity: 95.39% (C_{18} reverse phase, MeOH-H_2O, 70:30), 95.09% (C_{18} reverse phase, MeOH-H_2O, 75:25).

N-[6-(3-Aminopropyl)-11-hydroxy-5-oxo-6,11-dihydro-5*H*-indeno[1,2-*c*]isoquinolin-3-yl]acetamide (6)—

N-(6-(3-Aminopropyl)-5,11-dioxo-6,11-dihydro-5*H*indeno[1,2-*c*] isoquinolin-3-yl)acetamide (**5**, 252 mg, 0.70 mmol) was dissolved in methanol (30 mL) and the reaction mixture placed in the freezer for 1 h at −20 °C. The indenoisoquinoline solution was taken out of the freezer and placed in an ice bath at 0 °C. Sodium borohydride (0.80 g, 21 mmol) was added in two portions, stirring the reaction mixture for 15 min between each addition. A solution of ammonium chloride (200 mg) in water (50 mL) was added to the reaction mixture. Water (100 mL) was added to further dilute the solution and the desired compound was extracted with chloroform (6 × 20 mL). The organic extracts were combined and dried with sodium sulfate. The solvent was

removed under vacuum and compound **6** was obtained as a brown solid (92 mg, 36%): mp 300 °C (dec). IR (KBr) 3279, 3067, 2929, 2865, 1673, 1637, 1588, 1530, 1426, 1379, 1183, 1041, 956, 763, 743 cm^{-1}; ^1H NMR (500 MHz, DMSO-d_6) δ 10.20 (s, 1 H), 8.52 (d, J = 2.1 Hz, 1 H), 7.96-7.86 (m, 3 H), 7.61 (d, J = 7.0 Hz, 1 H), 7.40-7.33 (m, 2 H), 5.76 (d, J = 7.1 Hz, 1 H), 5.50 (s, 1 H), 4.51 (t, J = 7.4 Hz, 2 H), 2.65 (t, J = 6.6 Hz, 2 H), 1.98 (s, 3 H), 1.80 (m, 2 H); ^{13}C NMR (125 MHz, DMSO-d_6) δ 168.8, 162.4, 148.7, 138.5, 138.1, 135.4, 129.8, 129.0, 127.7, 125.1, 124.7, 124.6, 124.5, 122.0, 120.8, 117.0, 71.2, 41.7, 32.7, 24.4; ESIMS *m/z* (rel intensity) 364 (MH^+, 100); HRESIMS *m/z* expected for $C_{21}H_{21}N_3O_3$ 364.1661 (MH^+), found 364.1666 (MH^+); HPLC purity: 95.65% (C_{18} reverse phase, MeOH, 100).

6-(3-Hydroxypropyl)-3-amino-5*H*-indeno[1,2-*c*]isoquinoline-5,11(6*H*)dione (7)— 6-(3-Hydroxypropyl)-3-nitro-5*H*-indeno[1,2-*c*]isoquinoline-5,11(6*H*)-dione (**23**, 301 mg, 0.68 mmol) was dissolved in ethanol (20 mL) and water (5 mL). Iron powder (300 mg) and ammonium chloride (50 mg) were added and the reaction mixture was stirred at reflux for 3 h. Sodium hydroxide (50 mg) was added and the reaction mixture heated at reflux for 30 min. The solvent was removed and the compound was purified by silica gel column chromatography, eluting with chloroform-methanol, 10:1. The title compound **7** was obtained as a brown solid (229 mg, 83.0 %): mp 236–238 °C. IR (neat) 3383, 3311, 3057, 2934, 2921, 1703, 1649, 1579, 1465, 1333, 1307, 1275, 1192, 1057, 899 cm^{-1}; ^1H NMR (300 MHz, DMSO-d_6) δ 8.25 (d, J = 8.6 Hz, 1 H), 7.79 (d, J = 7.4 Hz, 2 H), 7.45 (m, 2 H), 7.32 (m, 2 H), 7.07 (dd, J = 8.7 Hz, J = 2.3 Hz, 1 H), 4.85 (br t, J = 4.7 Hz, 1 H), 4.64 (br t, J = 8.3 Hz, 1 H), 3.61 (br q, J = 5.2 Hz, J = 5.7 Hz, 2 H), 1.91 (m, 2 H); ^{13}C NMR (75 MHz, $CDCl_3$) δ 190.9, 164.1, 151.4, 146.1, 137.5, 134.7, 133.3, 130.1, 125.0, 124.8, 124.1, 123.1, 123.0, 121.8, 110.8, 109.9, 58.2, 40.9, 32.3; ESIMS *m/z* (rel intensity) 321 (MNa^+, 100); HRESIMS *m/z* expected for $C_{19}H_{16}N_2O_3$ 321.1239 (MH^+), found 321.1242 (MH^+); HPLC purity: 95.67 % (C_{18} reverse phase, MeOH-H_2O, 80:20), 97.27 % (C_{18} reverse phase, MeOH-H_2O, 70:30).

3-Amino-11-hydroxy-6-(3-hydroxypropyl)-6,11-dihydro-5*H*-indeno[1,2-*c*]isoquinolin-5-one (8)—3-Amino-6-(3-hydroxypropyl)-5*H*-indeno[1,2-*c*]isoquinoline-5,11(6*H*)-dione (**7**, 80 mg, 0.25 mmol) was dissolved in methanol (15 mL) and the reaction mixture was cooled to 0 °C. Sodium borohydride (361 mg, 9.55 mmol) was added in portions and the reaction mixture was stirred for 30 min, keeping the temperature constant. The reaction mixture went from a light purple color to a yellow color and constant bubbling was observed. An extra amount of sodium borohydride (365 mg, 9.65 mmol) was added after 10 min. A solution of saturated ammonium chloride (50 mL) was added and the reaction mixture extracted with dichloromethane (5 × 20 mL) until the organic phase was colorless. The organic extracts were washed with brine (40 mL) and dried over sodium sulfate. The solvent was removed in vacuo and the solid residue was washed with hexane (10 mL) and filtered. The product **8** was obtained as a light brown solid (49 mg, 61%): mp 148–150 °C. IR (neat) 3349, 2922, 1623, 1573, 1517, 1378, 1261, 876, 758, 742 cm^{-1}; ^1H NMR (300 MHz, DMSO-d_6) δ 7.86 (d, J = 7.5 Hz, 1 H), 7.78 (d, J = 8.5 Hz, 1 H), 7.39-7.28 (m, 3 H), 7.06 (d, J = 8.4 Hz, 1 H), 5.69-5.64 (m, 3 H), 5.44 (d, J = 8.5 Hz, 1 H), 4.50 (br t, J = 7.7 Hz, 2 H), 3.61 (br q, J = 5.0 Hz, 2 H), 1.90 (br s, 2 H); ^{13}C NMR (75 MHz, DMSO-d_6) δ 162.8, 148.9, 148.8, 136.7, 135.6, 129.4, 127.3, 126.4, 125.9, 125.5, 125.0, 122.4, 121.8, 121.7, 110.0, 72.0, 59.4, 42.2, 33.1; EIMS *m/z* (rel intensity): 323 (MH^+, 100); HRESIMS *m/z* expected for $C_{19}H_{18}N_2O_3$ 323.1396 (MH^+), found 323.1400 (MH^+); HPLC purity: 96.51% (C_{18} reverse phase, MeOH-H_2O, 60:40), 98.09% (C_{18} reverse phase, MeOH-H_2O, 90:10).

***N*-[6-(3-Hydroxypropyl)-5,11-dioxo-6,11-dihydro-5*H*-indeno[1,2-*c*]isoquinolin-3-yl]acetamide (9)—**6-(3-Bromopropyl)-3-nitro-5*H*-indeno[1,2-*c*] isoquinoline-5,11(6*H*)-dione (**24**, 1.01 g, 2.44 mmol) was dissolved in ethanol (50 mL). Iron power (682 mg, 12.2 mmol) was added to the reaction vessel. Ammonium chloride (53 mg, 1.0 mmol) was dissolved in water (10 mL) and added to the reaction mixture. The reaction mixture was heated at reflux for 3 h. Concentrated hydrochloric acid (1 mL) was added and the reaction mixture heated at reflux for 30 min. The reaction mixture was cooled to room temperature and a solution of sodium hydroxide (381 mg) in water (10 mL) was added. The reaction mixture was heated at reflux for 30 min, filtered, and the solid washed with tetrahydrofuran (50 mL). The solution was concentrated and the solid residue dissolved in tetrahydrofuran (50 mL) and cooled to 0 °C. Acetyl chloride (1 mL) was added and the reaction mixture was stirred for 30 min at 0 °C, and then sodium hydroxide (400 mg) was added. The reaction mixture was allowed to warm to room temperature and stirred for 1 h. The reaction mixture was then heated at reflux for 1 h. Chloroform (150 mL) was added and the organic phase washed with saturated ammonium chloride (50 mL) and water (3 × 100 mL). The organic solvent was removed in vacuo and the residue purified by silica gel column chromatography, eluting with chloroform to chloroform-methanol, 10:1. The product **9** was obtained as a red solid (387 mg, 43.7%): mp 265-267 °C. IR (neat) 3343, 1708, 1674, 1631, 1565, 1428, 1323, 1274, 1197, 903, 842, 765 cm^{-1}; ^1H NMR (500 MHz, DMSO-d_6) δ 10.26 (s, 1 H), 8.50 (s, 1 H), 8.43 (d, J = 8.7 Hz, 1 H), 7.91-7.87 (m, 2 H), 7.51-7.48 (m, 2 H), 7.71 (d, J = 7.1 Hz, 1 H), 4.85 (s, 1 H), 4.48 (t, J = 7.8 Hz, 2 H), 3.60 (br q, J = 5.3 Hz, 2 H), 2.05 (s, 3 H) 1.92 (m, 2 H); ^{13}C NMR (125 MHz, DMSO-d_6) δ 190.3, 168.9, 162.5, 155.0, 138.6, 137.1, 134.7, 134.2, 131.2, 127.4, 125.8, 123.9, 123.8, 123.6, 122.8, 116.8, 107.4, 58.6, 42.8, 32.1, 24.4; APCIMS *m/z* (rel intensity) 363 (MH^+, 100); HRCIMS *m/z* expected for $C_{21}H_{18}N_2O_4$ 362.1267 (M^+), found 362.1260 (M^+); HPLC purity: 95.81 % (C_{18} reverse phase, MeOH-H_2O, 75:25); 95.27 % (C_{18} reverse phase, MeOH-H_2O, 80:20).

3-Amino-6-(3-chloropropyl)-5,6-dihydro-5,11-dioxo-11*H*-indeno[1,2-*c*]isoquinoline (12)—6-(3-Chloropropyl)-5,6-dihydro-3-nitro-5,11-dioxo-11*H*-indeno[1,2-*c*]isoquinoline (**11**) (0.44 g, 1.19 mmol) and 10% Pd-C (100 mg) were diluted with tetrahydrofuran (25 mL) and methanol (25 mL). The reaction mixture was placed in a Parr shaker and stirred under a hydrogen atmosphere (50 psi) for 12 h. The solution was heated to reflux and filtered immediately, the filter pad was washed with hot chloroform-methanol, 1:1 (150 mL), and the filtrate was concentrated to provide a crude purple solid that was purified by silica gel column chromatography, eluting with chloroform-methanol, 20:1, to provide a brown solid (0.384 g, 95.4%): mp 194–196 °C. IR (KBr) 3358, 1703, 1641, 1577, 1517 cm^{-1}; ^1H NMR (500 MHz, DMSO-d_6) δ 8.40 (d, J = 8.6 Hz, 1 H), 7.74 (d, J = 7.6 Hz, 1 H), 7.63 (s, 1 H), 7.55-7.32 (m, 4 H), 4.59 (t, J = 6.8 Hz, 2 H), 3.90 (t, J = 6.4 Hz, 2 H), 2.27 (m, 2 H); ^{13}C NMR (125 MHz, DMSO-d_6) δ 190.8, 169.5, 163.1, 155.3, 139.2, 137.5, 135.1, 134.7, 131.8, 127.9, 127.0, 124.1, 124.0, 123.4, 117.2, 108.1, 43.7, 43.1, 32.5, 24.9; EIMS *m/z* (rel intensity) 338 (M^+, 100), 340 (M^+, 36); HREIMS *m/z* expected for $C_{19}H_{15}ClN_2O_2$ 338.0822 (M^+), found 338.0828 (M^+). Anal. calcd for $C_{19}H_{15}ClN_2O_2 \cdot 0.3\ H_2O$: C, 66.30; H, 4.57; N, 8.14; found: C, 66.20; H, 4.59; N, 7.86.

***N*-[6-(3-Chloropropyl)-5,11-dioxo-6,11-dihydro-5*H*-indeno[1,2-*c*]isoquinolin-3-yl]acetamide (13)—**3-Amino-6-(3-chloropropyl)-5,6-dihydro-5,11-dioxo-11*H*-indeno[1,2-*c*]isoquinoline (**12**, 781 mg, 2.31 mmol) was dissolved in dry tetrahydrofuran (20 mL). The reaction mixture was cooled to 0 °C and acetyl chloride (0.5 mL) was added. The reaction mixture was stirred for 1 h and then diluted with chloroform (30 mL). The organic phase was washed with water and brine (30 mL each) and the solvent removed in vacuo. A red solid was obtained and purified by silica gel column chromatography, eluting with chloroform-methanol-triethylamine, 20:1:0.5. The product **13** was obtained as a red solid

(662 mg, 74.8%): mp 237–240 °C. IR (neat) 3365, 3331, 2968, 1697, 1668, 1639, 1569, 1507,1431, 1303,1196, 904, 850, 761 cm^{-1}; ^1H NMR (300 MHz, DMSO-d_6) δ 10.30 (s , 1 H), 8.54 (d, *J* = 2.2 Hz, 1 H), 8.46 (d, *J* = 8.8 Hz, 1 H), 7.94 (dd, *J* = 8.8 Hz, *J* = 2.3 Hz, 1 H), 7.77 (d, *J* = 7.4 Hz, 1 H), 7.58-7.42 (m, 3 H), 4.58 (t, *J* = 8.0 Hz, 2 H), 3.88 (t, *J* = 6.4 Hz, 2 H), 2.28 (m, 2 H); ^{13}C NMR (75 MHz, DMSO-d_6) δ 190.8, 169.5, 163.1, 155.3, 139.2, 137.5, 135.1, 134.7, 131.8, 127.9, 126.3, 124.3, 124.1, 123.9, 123.4, 117.2, 108.1, 43.7, 43.1, 32.5, 24.9; ESIMS *m/z* (rel intensity) 405 (MNa^+ 15), 403 (MNa^+ 44), 383 (MH^+, 43), 381 (MH^+, 100); HPLC purity: 95.57% (C_{18} reverse phase, MeOH-H_2O, 90:10), 95.42% (C_{18} reverse phase, MeOH-H_2O, 95:5). Anal. calcd for $C_{21}H_{17}ClN_2O_3 \cdot 0.5\ H_2O$: C, 64.70; H, 4.65; N, 7.19; found: C, 64.61; H, 4.63; N, 7.11.

N*-[6-(3-Azidopropyl)-5,11-dioxo-6,11-dihydro-5*H*-indeno[1,2-*c*]isoquinolin-3-yl]acetamide (14)—N*-(6-(3-Chloropropyl)-5,11-dioxo-6,11-dihydro-5*H*-indeno[1,2-*c*]isoquinolin-3-yl)acetamide (**13**, 400 mg, 1.05 mmol) was dissolved in dimethylsulfoxide (50 mL). Sodium azide (200 mg, 3.07 mmol) was added and the solution was heated for 8 h at 100 °C. The reaction mixture was diluted with water (200 mL) and extracted with chloroform (5 × 50 mL). The organic extracts were combined and washed with water (4 × 100 mL). The solvent was removed in vacuo and the compound purified by silica gel column chromatography, eluting with chloroform-methanol, 20:1. The solvent was removed in vacuo and the residue was recrystallized from chloroform-methanol giving a dark pink solid (299 mg, 75.6%): mp 216–217 °C. IR (neat) 3072, 2923, 2858, 2099, 1663, 1572, 1532, 1512, 1433, 1304, 1274, 1195, 843, 760 cm^{-1}; ^1H NMR (300 MHz, DMSO-d_6) δ 10.1 (s, 1 H), 8.41 (d, *J* = 2.0 Hz, 1 H), 8.27 (d, *J* = 8.7 Hz, 1 H), 7.79 (dd, *J* = 8.8 Hz, *J* = 2.2 Hz, 1 H), 7.61 (d, *J* = 7.5 Hz, 1 H), 7.47-737 (m, 3 H), 4.41 (t, *J* = 7.5 Hz, 2 H), 3.59 (t, *J* = 6.5 Hz, 2 H), 2.03-1.97 (m, 5 H); ^{13}C NMR (75 MHz, DMSO-d_6) δ 190.7, 169.4, 155.1, 139.2, 137.5, 135.1, 134.6, 131.7, 127.8, 126.2, 124.3, 124.1, 123.9, 123.3, 117.1, 108.1, 49.4, 42.8, 29.1, 24.9; ESIMS *m/z* (rel intensity) 410 (MNa^+ 100); HRESIMS *m/z* expected for $C_{21}H_{17}N_5O_3$ 410.1229 (MNa^+), found 410.1232 (MNa^+); HPLC purity: 96.92% (C_{18} reverse phase, MeOH-H_2O, 85:15), 98.83% (C_{18} reverse phase, MeOH-H_2O, 80:20).

***tert*-Butyl 3-(3-Nitro-5,11-dioxo-5*H*-indeno[1,2-*c*]isoquinolin-6(11*H*)-yl)propylcarbamate (16)—**6-(3-Aminopropyl)-3-nitro-5*H*-indeno[1,2-*c*]isoquinoline-5,11(6*H*)-dione hydrochloride (**15**, 385 mg, 1.00 mmol) and triethylamine (0.12 mL) were dissolved in methanol (15 mL) and the reaction mixture was cooled to 0 °C. Di-*tert*-butyl dicarbonate (300 mg, 1.37 mmol) was slowly added and the reaction mixture stirred overnight at room temperature. The solvent was removed in vacuo and the residue purified by silica gel column chromatography, eluting with chloroform-methanol, 30:1. The product was obtained as a yellow solid (415 mg, 92.4%): mp 245–247 °C. IR (neat) 3359, 2981, 2941, 1706, 1678, 1665, 1617, 1523, 1504, 1424, 1331, 1165, 998, 848, 785, 741 cm^{-1}; ^1H NMR (300 MHz, $CDCl_3$) δ 9.20 (s, 1 H), 8.87 (d, *J* = 8.9 Hz, 1 H), 8.48 (d, *J* = 8.8 Hz, 1 H), 7.71-7.65 (m, 2 H), 7.53-7.49 (m, 2 H), 5.20 (s, 1 H), 4.67 (t, *J* = 7.2 Hz, 2 H), 3.30 (t, *J* = 4.6 Hz, 2 H), 2.21 (t, *J* = 7.0 Hz, 2 H), 1.46 (s, 9 H); ESIMS (rel intensity) *m/z* 472 (MNa^+ 100); HRESIMS *m/z* expected for $C_{24}H_{23}N_3O_6$ 472.1485 (MNa^+), found 472.1482 (MNa^+); HPLC purity: 96.39% (C_{18} reverse phase, MeOH-H_2O, 90:10), 96.45% (C_{18} reverse phase, MeOH, 100).

tert*-Butyl 3-(3-Amino-5,11-dioxo-5*H*-indeno[1,2-*c*]isoquinolin-6(11*H*)-yl) propylcarbamate (17)—tert*-Butyl 3-(3-nitro-5,11-dioxo-5*H*-indeno[1,2-*c*]isoquinolin-6(11*H*)-yl)propylcarbamate (**16**, 200 mg, 0.44 mmol) was dissolved in methanol (25 mL) and chloroform (25 mL). 10% Pd-C (15 mg) was added and the reaction mixture placed in a Parr shaker. Hydrogen (50 psi) was applied to the reaction vessel and the suspension was shaken overnight at room temperature. The palladium catalyst was filtered

off and the compound purified by silica gel column chromatography, eluting with chloroform-methanol, 10:1. Compound **17** was obtained as a dark-brown solid (145 mg, 76%): mp 328–330 °C. IR (neat) 3173, 3005, 2958, 2933, 2872, 1704, 1627, 1590, 1554, 1477, 1425, 1326, 1168, 1043, 875 cm^{-1}; ^1H NMR (300 MHz, $CDCl_3$) δ 8.24 (d, *J* = 8.6 Hz, 1 H), 7.56 (d, *J* = 7.6 Hz, 1 H), 7.47-7.31 (m, 4 H), 7.07 (d, *J* = 8.6 Hz, 1 H), 7.01 (br t, 1 H), 5.7 (s, 2 H), 4.38 (t, *J* = 7.1 Hz, 2 H), 3.09 (q, *J* = 6.1 Hz, 2 H), 1.85 (t, 2 H), 1.37 (s, 9 H); ^{13}C NMR (75 MHz, $CDCl_3$) δ 190.8, 162.4, 156.0, 151.3, 148.9, 137.8, 134.6, 134.0, 130.4, 125.1, 124.1, 122.7, 122.6, 122.4, 121.4, 109.2, 108.6, 78.0, 42.4, 37.8, 30.1, 28.6; ESIMS *m/z* (rel intensity) 442 (MNa^+ 100); HRESIMS *m/z* expected for $C_{24}H_{25}N_3O_4$ 420.1923 (MH^+) found 420.1919 (MH^+); HPLC purity 95.62% (C_{18} reverse phase, MeOH-H_2O, 80:20), 95.24% (C_{18} reverse phase, MeOH-H_2O, 90:10).

***N*-[3-(3-Nitro-5,11-dioxo-5*H*-indeno[1,2-*c*]isoquinolin-6(11*H*)-yl)propyl]acetamide(19)—**6-(3-Aminopropyl)-3-nitro-5*H*-indeno[1,2-*c*]isoquinoline-5,11(6*H*)-dione hydrochloride (**15**, 240 mg, 0.624 mmol) was dissolved in tetrahydrofuran (20 mL) and the reaction mixture was cooled to 0 °C. Acetyl chloride (0.6 mL) and triethylamine (0.3 mL) were added and the reaction mixture was stirred for 1 h at room temperature. Water (60 mL) was added and the resulting solution extracted with chloroform (3 × 40 mL). The chloroform was removed and the solid dissolved in hot chloroform-dimethylformamide, 9:1 (20 mL). The reaction mixture was allowed to reach room temperature, ethyl ether (25 mL) was added and the reaction mixture was placed in the freezer overnight. The indenoisoquinoline **19** was obtained as an orange solid (211 mg, 93.1%): mp 291–293 °C. IR (neat) 3434, 1663, 1646, 1496, 1423, 1334, 863, 787, 749 cm^{-1}; ^1H NMR (500 MHz, DMSO-d_6) δ 8.89 (s , 1 H), 8.67 (s, 1 H), 8.54 (dd, *J* = 6.5 Hz, *J* = 2.5 Hz, 1 H), 8.04 (s, 1 H), 7.79 (d, *J* = 7.5 Hz, 1 H), 7.62-7.58 (m, 2 H), 7.56 (d, *J* = 7.6 Hz, 1 H), 4.47 (t, *J* = 7.0 Hz, 2 H), 3.22 (q, *J* = 6.7 Hz, *J* = 6.2 Hz, 2 H), 1.91 (t, *J* = 7.3 Hz, 2 H), 1.89 (s, 3 H); ^{13}C NMR (125 MHz, DMSO-d_6) δ 189.6, 169.7, 162.3, 159.5, 145.4, 136.7, 134.9, 134.6, 132.7, 128.3, 124.9, 124.4, 124.3, 123.5, 122.8, 106.7, 43.3, 36.3, 29.3, 22.9; ESIMS *m/z* (rel intensity) 392 (MH^+, 65), 349 ([MH - C_2H_3O]$^+$, 100); HRESIMS *m/z* expected for $C_{21}H_{17}N_3O_5$ 392.1246 (MH^+) found 392.1241 (MH^+); HPLC purity: 95.03% (C_{18} reverse phase, MeOH-H_2O, 90:10), 97.12% (C_{18} reverse phase, MeOH-H_2O, 95:5).

***N*-[3-(3-Amino-5,11-dioxo-5*H*-indeno[1,2-*c*]isoquinolin-6(11*H*)-yl)propyl]acetamide (20)—**6-(3-Aminopropyl)-3-nitro-5*H*-indeno[1,2-*c*]isoquinoline-5,11(6*H*)-dione (**19**, 230 mg, 0.66 mmol) was dissolved in hot tetrahydrofuran (10 mL) and dimethylformamide (5 mL) and the solution was transferred to a Parr-shaker flask. A mixture of methanol (20 mL) and tetrahydrofuran (20 mL) was added to the vessel. The vessel was purged with argon for 10 min and then 10% Pd-C (100 mg) was added. The reaction mixture was stirred for 8 h under an atmosphere of hydrogen (60 psi). Water (50 mL) was added and the compound extracted with chloroform (4 × 20 mL). The chloroform extracts were washed with water (5 × 30 mL) and brine (50 mL). The compound was purified by silica gel column chromatography, eluting with chloroform-methanol, 20:1. The compound was obtained as a brick-red solid (163 mg, 68.4%): mp 221 °C (dec). IR (neat) 3334, 3073, 2928, 1698, 1646, 1577, 1515, 1429, 1364, 1317, 1195, 901, 784, 760 cm^{-1}; ^1H NMR (500 MHz, DMSO-d_6) δ 8.30 (d, *J* = 8.6 Hz, 1 H), 8.06 (br t, 1 H), 7.57 (d, *J* = 7.6 Hz, 1 H), 7.50 (d, *J* = 2.0 Hz, 1 H), 7.47-7.44 (m, 2 H), 7.36 (d, *J* = 7.4 Hz, 1 H), 7.21 (dd, *J* = 6.4 Hz, *J* = 2.3 Hz, 1 H), 4.38 (t, *J* = 6.1 Hz, 2 H), 3.17 (dd, *J* = 6.2 Hz, *J* = 6.7 Hz, 2 H), 1.85 (t, *J* = 7.7 Hz, 2 H), 1.80 (s, 3 H); ^{13}C NMR (125 MHz, DMSO-d_6) δ 190.6, 169.6, 162.3, 152.6, 137.5, 134.6, 134.2, 130.7, 124.7, 124.3, 124.0, 123.0, 122.8, 112.4, 108.3, 42.6, 36.4, 29.7, 23.0; ESIMS *m/z* (rel intensity) 362 (MH^+, 100); HRESIMS *m/z* expected for $C_{21}H_{19}N_3O_3$ 362.1508 (MH^+), found 362.1509 (MH^+); HPLC purity:

97.76% (C_{18} reverse phase, MeOH-H_2O, 80:20), 96.43% (C_{18} reverse phase, MeOH-H_2O, 90:10).

6-(3-Hydroxypropyl)-3-nitro-5*H*-indeno[1,2-*c*]isoquinoline-5,11(6*H*)dione (23)— 3-Nitroindeno[1,2-*c*]isochromene-5,11-dione (**21**, 200 mg, 0.68 mmol) was dissolved in chloroform (20 mL). A solution of 3-amino-1-propanol (**22**, 191 mg, 2.55 mmol) in chloroform (5 mL) was added dropwise. The reaction mixture was stirred for 5 min at room temperature and then it was heated at reflux for 8 h. The solvent was removed in vacuo and the compound was purified by silica gel column chromatography, eluting with chloroform-methanol, 20:1. The product **23** was obtained as a red solid (163 mg, 68.1%): mp 245–247 °C. IR (neat) 3390, 3094, 2947, 1670, 1612, 1581, 1558, 1503, 1428, 1335 cm^{-1}; ^1H NMR (500 MHz, $CDCl_3$) δ 9.21 (d, *J* = 2.4 Hz, 1 H), 8.88 (d, *J* = 8.9 Hz, 1 H), 8.51 (dd, *J* = 2.4 Hz, *J* = 8.9 Hz, 1 H), 7.87 (d, *J* = 7.6 Hz, 1 H), 7.72 (dd, *J* = 1.1 Hz, *J* = 7.9 Hz, 1 H), 7.55-750 (m, 2 H), 4.76 (t, *J* = 7.0 Hz, 2 H), 3.81 (t, *J* = 5.4 Hz, 2 H), 2.65 (m, 1 H), 2.18 (t, *J* = 5.2 Hz, 2 H); ^{13}C NMR (125 MHz, $CDCl_3$) δ 199.1, 163.2, 158.1, 145.8, 136.6, 135.9, 134.9, 133.8, 132.2, 127.8, 124.9, 124.7, 123.9, 123.8, 122.9, 107.7, 58.8, 42.2, 31.2; ESIMS *m/z* (rel intensity) 349 (M - H^+, 100); HRESIMS *m/z* expected for $C_{19}H_{14}N_2O_5Cl$ 385.0591 [(M + Cl)$^-$], found 385.0595 [(M + Cl)$^-$]; HPLC purity: 95.87 % (C_{18} reverse phase, MeOH-H_2O, 90:10), 97.40 % (C_{18} reverse phase, MeOH-H_2O, 95:5).

Supplementary Material

Refer to Web version on PubMed Central for supplementary material.

Acknowledgments

This work was facilitated by the National Institutes of Health (NIH) through support with Research Grant P01 CA48112. This work was also supported by the NIH, National Cancer Institute R25CA128770 (D. Teegarden) Cancer Prevention Internship Program (M.C.-S.) administered by the Oncological Sciences Center and the Discovery Learning Research Center at Purdue University. M.C.-S. thanks Dr. Karl Wood and Dr. Huaping Mo for consultation and valuable discussion.

Abbreviations

9cRA	9-*cis*-retinoic acid
APCIMS	atmospheric pressure chemical ionizationmass spectrometry
BBO	multinuclear broadband observe
DMSO	dimethylsulfoxide
EC_{50}	half maximal effective concentration, the concentration needed to induce a response that is equal to half the maximum response
EIMS	electron impact mass spectrometry
ESIMS	electrospray ionization mass spectrometry
LC-MS/MS	high performance liquid chromatography-tandem mass spectrometry
QNP	quattro nucleus probe
p21	cyclin-dependent kinase inhibitor 1
RXR	retinoid X receptor
RXRE	retinoid X receptor response element.

References

1. Mangelsdorf DJ, Thummel C, Beato M, Herrlich P, Schutz G, Umesono K, Blumberg B, Kastner P, Mark M, Chambon P, Evans RM. The Nuclear Receptor Superfamily - the ^{2nd} Decade. Cell. 1995; 83:835–839. [PubMed: 8521507]
2. Yu VC, Delsert C, Andersen B, Holloway JM, Devary OV, Naar AM, Kim SY, Boutin JM, Glass CK, Rosenfeld MG. RXRβ: a Coregulator that Enhances Binding of Retinoic Acid, Thyroid Hormone, and Vitamin D Receptors to Their Cognate Response Elements. Cell. 1991; 67:1251–1266. [PubMed: 1662118]
3. Wagner CE, Jurutka PW, Marshall PA, Groy TL, van der Vaart A, Ziller JW, Furmick JK, Graeber ME, Matro E, Miguel BV, Tran IT, Kwon J, Tedeschi JN, Moosavi S, Danishyar A, Philp JS, Khamees RO, Jackson JN, Grupe DK, Badshah SL, Hart JW. Modeling, Synthesis and Biological Evaluation of Potential Retinoid X Receptor (RXR) Selective Agonists: Novel Analogues of 4-[1-(3,5,5,8,8-Pentamethyl-5,6,7,8-tetrahydro-2-naphthyl)ethynyl]benzoic Acid (Bexarotene). J. Med. Chem. 2009; 52:5950–5966. [PubMed: 19791803]
4. Rastinejad F. Retinoid X Receptor and Its Partners in the Nuclear Receptor Family. Curr. Opin. Struct. Biol. 2001; 11:33–38. [PubMed: 11179889]
5. Mangelsdorf DJ, Evans RM. The RXR Heterodimers and Orphan Receptors. Cell. 1995; 83:841–850. [PubMed: 8521508]
6. Tanaka T, Suh KS, Lo AM, De Luca LM. P21$^{(WAF1/CIP1)}$ Is a Common Transcriptional Target of Retinoid Receptors. J. Biol. Chem. 2007; 282:29987–29997. [PubMed: 17656367]
7. Teplitzky SR, Kiefer TL, Cheng Q, Dwivedi PD, Moroz K, Myers L, Anderson MB, Collins A, Dai J, Yuan L, Spriggs LL, Blask DE, Hill SM. Chemoprevention of NMU-Induced Rat Mammary Carcinoma with the Combination of Melatonin and 9-*cis*-Retinoic Acid. Cancer Lett. 2001; 168:155–163. [PubMed: 11403920]
8. Teplitzky SR, Blask DE, Cheng Q, Myers L, Hill SM. Melatonin and 9-*cis*-Retinoic Acid in the Chemoprevention of NMU-Induced Rat Mammary Carcinoma. Adv. Exp. Biol. Med. 1999; 460:363–367.
9. Zanardi S, Serrano D, Argusti A, Barile M, Puntoni M, Decensi A. Clinical Trials with Retinoids for Breast Cancer Chemoprevention. Endocr.-Relat. Cancer. 2006; 13:51–68. [PubMed: 16601279]
10. Lee HY, Chang YS, Han JY, Liu DD, Lee JJ, Lotan R, Spitz MR, Hong WK. Effects of 9-*cis*-Retinoic Acid on the Insulin-like Growth Factor Axis in Former Smokers. J. Clin. Oncol. 2005; 23:4439–4449. [PubMed: 15994153]
11. Zusi FC, Lorenzi MV, Vivat-Hannah V. Selective Retinoids and Rexinoids in Cancer Therapy and Chemoprevention. Drug Discov. Today. 2002; 7:1165–1174. [PubMed: 12547017]
12. Alvarez RD, Conner MG, Weiss H, Klug PM, Niwas S, Manne U, Bacus J, Kagan V, Sexton KC, Grubbs CJ, Eltoum IE, Grizzle WE. The Efficacy of 9-*cis*-Retinoic Acid (Aliretinoin) As a Chemopreventive Agent for Cervical Dysplasia: Results of a Randomized Double-blind Clinical trial. Cancer Epidemiol. Biomarkers Prev. 2003; 12:114–119. [PubMed: 12582020]
13. Ruzicka T, Lynde CW, Jemec GBE, Diepgen T, Berth-Jones J, Coenraads PJ, Kaszuba A, Bissonnette R, Varjonen E, Hollo P, Cambazard F, Lahfa M, Elsner P, Nyberg F, Svensson A, Brown TC, Harsch M, Maares J. Efficacy and Safety of Oral Alitretinoin (9-*cis*-Retinoic Acid) in Patients with Severe Chronic Hand Eczema Refractory to Topical Corticosteroids: Results of a Randomized, Double-Blind, Placebo-Controlled, Multicentre trial. Br. J. Dermatol. 2008; 158:808–817. [PubMed: 18294310]
14. Ponthan F, Kogner P, Bjellerup P, Klevenvall L, Hassan M. Bioavailability and Dose-Dependent Anti-Tumour Effects of 9-*cis*-Retinoic Acid on Human Neuroblastoma Xenografts in Rat. Br. J. Cancer. 2001; 85:2004–2009. [PubMed: 11747346]
15. Miller WH, Jakubowski A, Tong WP, Miller VA, Rigas JR, Benedetti F, Gill GM, Truglia JA, Ulm E, Shirley M, Warrell RP. 9-cis-Retinoic Acid Induces Complete Remission but Does Not Reverse Clinically Acquired Retinoid Resistance in Acute Promyelocytic Leukemia. Blood. 1995; 85:3021–3027. [PubMed: 7756637]
16. de Lera AR, Bourguet W, Altucci L, Gronemeyer H. Design of Selective Nuclear Receptor Modulators: RAR and RXR As a Case Study. Nat. Rev. Drug Discovery. 2007; 6:811–820.

17. Altucci L, Leibowitz MD, Ogilvie KM, de Lera AR, Gronemeyer H. RAR and RXR Modulation in Cancer and Metabolic Disease. Nat. Rev. Drug Discovery. 2007; 6:793–810.
18. Esteva FJ, Glaspy J, Baidas S, Laufman L, Hutchins L, Dickler M, Tripathy D, Cohen R, DeMichele A, Yocum RC, Osborne CK, Hayes DF, Hortobagyi GN, Winer E, Demetri GD. Multicenter Phase II Study of Oral Bexarotene for Patients with Metastatic Breast Cancer. J. Clin. Oncol. 2003; 21:999–1006. [PubMed: 12637463]
19. Sherman SI, Gopal J, Haugen BR, Chiu AC, Whaley K, Nowlakha P, Duvic M. Central Hypothyroidism Associated with Retinoid X Receptor-Selective Ligands. New Engl. J. Med. 1999; 340:1075–1079. [PubMed: 10194237]
20. Gniadecki R, Assaf C, Bagot M, Dummer R, Duvic M, Knobler R, Ranki A, Schwandt P, Whittaker S. The Optimal Use of Bexarotene in Cutaneous T-cell Lymphoma. Br. J. Dermatol. 2007; 157:433–440. [PubMed: 17553039]
21. Sporn MB, Suh N. Chemoprevention: an Essential Approach to Controlling Cancer. Nat. Rev. Cancer. 2002; 2:537–543. [PubMed: 12094240]
22. Qu L, Tang X. Bexarotene: A Promising Anticancer Agent. Cancer Chemother. Pharmacol. 2010; 65:201–205. [PubMed: 19777233]
23. Park EJ, Kondratyuk TP, Morrell A, Kiselev E, Conda-Sheridan M, Cushman M, Ahn S, Choi Y, White JJ, van Breemen RB, Pezzuto JM. Induction of Retinoid X Receptor Activity and Consequent Upregulation of $p21^{(WAF1/CIP1)}$ by Indenoisoquinolines in MCF7 Cells. Cancer Prev. Res. 2011; 4:592–607.
24. Jahn U, Dinca E. Toward the Elucidation of the Metabolism of 15-E(2)-Isoprostane: The Total Synthesis of the Methyl Ester of a Potential Central Metabolite. J. Org. Chem. 2010; 75:4480–4491. [PubMed: 20527974]
25. Wu YS, Coumar MS, Chang JY, Sun HY, Kuo FM, Kuo CC, Chen YJ, Chang CY, Hsiao CL, Liou JP, Chen CP, Yao HT, Chiang YK, Tan UK, Chen CT, Chu CY, Wu SY, Yeh TK, Lin CY, Hsieh HP. Synthesis and Evaluation of 3-Aroylindoles as Anticancer Agents: Metabolite Approach. J. Med. Chem. 2009; 52:4941–4945. [PubMed: 19586033]
26. Xu DW, Penning TM, Blair IA, Harvey RG. Synthesis of Phenol and Quinone Metabolites of Benzo[*a*]pyrene, a Carcinogenic Component of Tobacco Smoke Implicated in Lung Cancer. J. Org. Chem. 2009; 74:597–604. [PubMed: 19132942]
27. Tiwari A, Riordan JM, Waud WR, Struck RF. Synthesis and Antitumor Activity of Several New Analogues of Penclomedine and Its Metabolites. J. Med. Chem. 2002; 45:1079–1085. [PubMed: 11855988]
28. Shin YG, Bolton JL, van Breemen RB. Screening Drugs for Metabolic Stability Using Pulsed Ultrafiltration Mass Apectrometry. Comb. Chem. High Throughput Screen. 2002; 5:59–64. [PubMed: 11860340]
29. Riley RJ, McGinnity DF, Austin RP. A Unified Model for Predicting Human Hepatic, Metabolic Clearance from In Vitro Intrinsic Clearance Data in Hepatocytes and Microsomes. Drug Metab. and Dispos. 2005; 33:1304–1311.
30. Wsól V, Kvasnicková E, Szotáková B, Hais IM. High-performance Liquid Chromatography Assay for the Separation and Characterization of Metabolites of the Potential Cytostatic Drug Oracine. J. Chromatogr. B. 1996; 681:169–175.
31. Nikolic D, Fan PW, Bolton JL, van Breemen RB. Screening for Xenobiotic Electrophilic Metabolites Using Pulsed Ultrafiltration-Mass Spectrometry. Comb. Chem. High Throughput Screen. 1999; 2:165–175. [PubMed: 10420970]
32. Morrell A, Placzek M, Parmley S, Grella B, Antony S, Pommier Y, Cushman M. Optimization of the Indenone Ring of Indenoisoquinoline Topoisomerase I Inhibitors. J. Med. Chem. 2007; 50:4388–4404. [PubMed: 17676830]
33. Bae JW, Cho YJ, Lee SH, Yoon COM, Yoon CM. A One-Pot Synthesis of *N*-Alkylaminobenzenes from Nitroaromatics: Reduction Followed by Reductive Amination Using $B_{10}H_{14}$. Chem Commun. 2000:1857–1858.
34. Shendage DM, Frohlich R, Haufe G. Highly Efficient Stereoconservative Amidation and Deamidation of Alpha-Amino Acids. Org. Lett. 2004; 6:3675–3678. [PubMed: 15469321]

35. Morrell A, Antony S, Kohlhagen G, Pommier Y, Cushman M. Synthesis of Benz[d]indeno[1,2-b]pyran-5,11-diones: Versatile Intermediates for the Design and Synthesis of Topoisomerase I Inhibitors. Bioorg. Med. Chem. Lett. 2006; 16:1846–1849. [PubMed: 16442283]
36. Morrell A, Placzek M, Parmley S, Antony S, Dexheimer TS, Pommier Y, Cushman M. Nitrated Indenoisoquinolines as Topoisomerase I Inhibitors: A Systematic Study and Optimization. J. Med. Chem. 2007; 50:4419–4430. [PubMed: 17696418]
37. Sauer R, El-Tayeb A, Kaulich M, Muller CE. Synthesis of Uracil Nucleotide Analogs with a Modified, Acyclic Ribose Moiety as P2Y(2) Receptor Antagonists. Bioorg. Med. Chem. 2009; 17:5071–5079. [PubMed: 19523835]
38. McNulty J, Nair JJ, Cheekoori S, Larichev V, Capretta A, Robertson AJ. Scope and Mechanistic Insights into the Use of Tetradecyl(trihexyl)phosphonium Bistriflimide: A Remarkably Selective Ionic Liquid Solvent for Substitution Reactions. Chem.–Eur. J. 2006; 12:9314–9322. [PubMed: 17009361]
39. Barney CL, Huber EW, McCarthy JR. A Convenient Synthesis of Hindered Amines and Alpha-Trifluoromethylamines from Ketones. Tetrahedron Lett. 1990; 31:5547–5550.
40. Mehta K, McQueen T, Neamati N, Collins S, Andreeff M. Activation of Retinoid Receptors RAR Alpha and RXR Alpha Induces Differentiation and Apoptosis, Respectively, in HL-60 Cells. Cell Growth Differ. 1996; 7:179–186. [PubMed: 8822201]
41. Chiba-Mizutani T, Miura H, Matsuda M, Matsuda Z, Yokomaku Y, Miyauchi K, Nishizawa M, Yamamoto N, Sugiura W. Use of New T-Cell-based Cell Lines Expressing Two Luciferase Reporters for Accurately Evaluating Susceptibility to Anti-human Immunodeficiency Virus Type 1 Drugs. J. Clin. Microbiol. 2007; 45:477–487. [PubMed: 17182760]
42. Rayet B, Gelinas C. Aberrant rel/nfkb Genes and Activity in Human Cancer. Oncogene. 1999; 18:6938–6947. [PubMed: 10602468]
43. Hoffmann A, Natoli G, Ghosh G. Transcriptional Regulation Via the NF-kappa B Signaling Module. Oncogene. 2006; 25:6706–6716. [PubMed: 17072323]
44. Hayden MS, Ghosh S. Signaling to NF-kappa B. Genes Dev. 2004; 18:2195–2224. [PubMed: 15371334]
45. Gilmore TD. Introduction to NF-kappa B: Players, Pathways, Perspectives. Oncogene. 2006; 25:6680–6684. [PubMed: 17072321]
46. Zhang ZQ, Rigas B. NF-kappa B, Inflammation and Pancreatic Carcinogenesis: NF-kappa B As a Chemoprevention Target (Review). Int. J. Oncol. 2006; 29:185–192. [PubMed: 16773199]
47. Dorai T, Aggarwal BB. Role of Chemopreventive Agents in Cancer Therapy. Cancer Lett. 2004; 215:129–140. [PubMed: 15488631]
48. Surh YJ. Transcription Factors in the Cellular Signaling Network as Prime Targets of Chempreventive Phytochemicals. Cancer Res. Treat. 2004; 36:275–286. [PubMed: 20368816]
49. Shen Q, Brown PH. Novel Agents for the Prevention of Breast Cancer: Targeting Transcription Factors and Signal Transduction Pathways. J. Mammary Gland Biol. Neoplasia. 2003; 8:45–73. [PubMed: 14587863]
50. Luqman S, Pezzuto JM. NF kappa B: A Promising Target for Natural Products in Cancer Chemoprevention. Phytother. Res. 2010; 24:949–963. [PubMed: 20577970]
51. Kelly D, Campbell JI, King TP, Grant G, Jansson EA, Coutts AGP, Pettersson S, Conway S. Commensal Anaerobic Gut Bacteria Attenuate Inflammation by Regulating Nuclear-Cytoplasmic Shuttling of PPAR-Gamma and RelA. Nat. Immunol. 2004; 5:104–112. [PubMed: 14691478]
52. Na SY, Kang BY, Chung SW, Han SJ, Ma XJ, Trinchieri G, Im SY, Lee JW, Kim TS. Retinoids Inhibit Interleukin-12 Production in Macrophages Through Physical Associations of Retinoid X Receptor and NF kappa B. J. Biol. Chem. 1999; 274:7674–7680. [PubMed: 10075655]
53. Liby KT, Yore MM, Sporn MB. Triterpenoids and Rexinoids as Multifunctional Agents for the Prevention and Treatment of Cancer. Nat. Rev. Cancer. 2007; 7:357–369. [PubMed: 17446857]
54. Singh T, Vaid M, Katiyar N, Sharma S, Katiyar SK. Berberine, an Isoquinoline Alkaloid, Inhibits Melanoma Cancer Cell Migration by Reducing the Expressions of Cyclooxygenase-2, Prostaglandin E(2) and Prostaglandin E(2) Receptors. Carcinogenesis. 2011; 32:86–92. [PubMed: 20974686]

55. McIntyre KW, Shuster DJ, Gillooly KM, Dambach DM, Pattoli MA, Lu P, Zhou XD, Qiu YP, Zusi FC, Burke JR. A Highly Selective Inhibitor of I kappa B Kinase, BMS-345541, Blocks Both Joint Inflammation and Destruction in Collagen-Induced Arthritis in Mice. Semin. Arthritis and Rheum. 2003; 48:2652–2659.

56. Iwatsubo T, Hirota N, Ooie T, Suzuki H, Shimada N, Chiba K, Ishizaki T, Green CE, Tyson CA, Sugiyama Y. Prediction of In Vivo Drug Metabolism in the Human Liver from In Vitro Metabolism Sata. Pharmacol. Ther. 1997; 73:147–171. [PubMed: 9131722]

57. Hoshino J, Park EJ, Kondratyuk TP, Marler L, Pezzuto JM, van Breemen RB, Mo SY, Li YC, Cushman M. Selective Synthesis and Biological Evaluation of Sulfate-Conjugated Resveratrol Metabolites. J. Med. Chem. 2010; 53:5033–5043. [PubMed: 20527891]

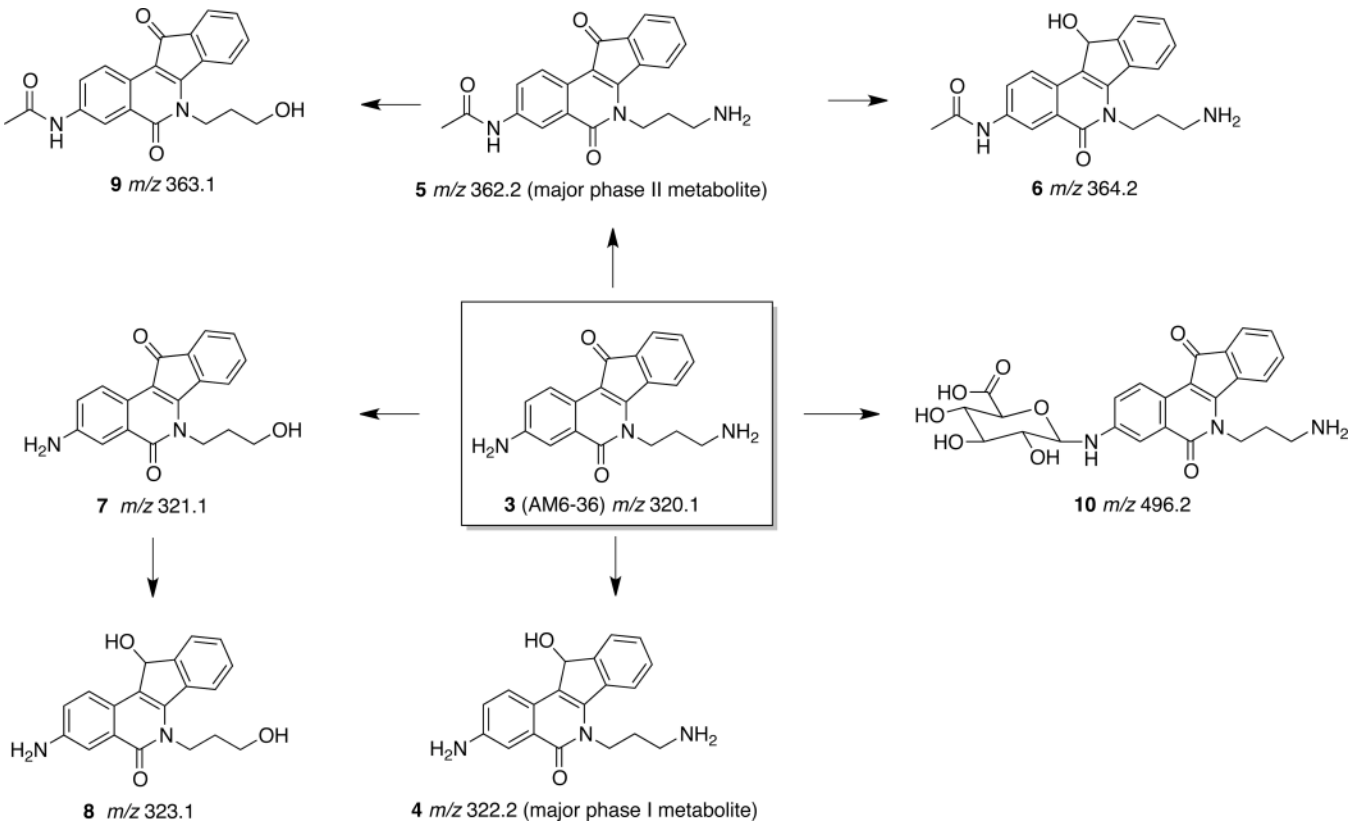

Figure 1.
Structures and proposed metabolic pathways of all 7 phase I and II human hepatic metabolites of **3**.

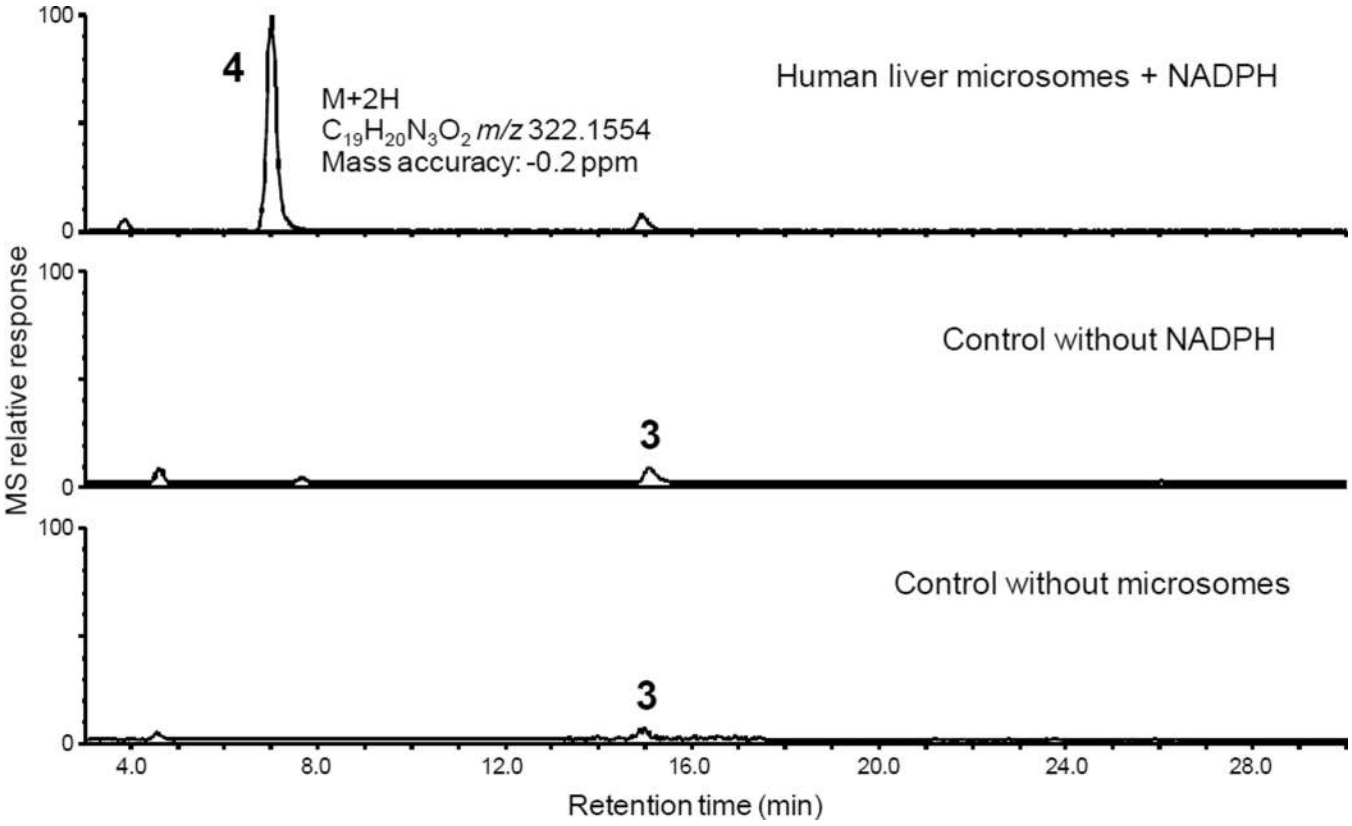

Figure 2.

Computer-reconstructed mass chromatograms of *m/z* 320 and *m/z* 322 from the high resolution positive ion electrospray LC-MS analysis of an incubation of **3** with pooled human liver microsomes. One phase I metabolite, **4**, was detected as a protonated molecule of *m/z* 322.1554 ($C_{19}H_{20}N_3O_2$, ΔM −0.2 ppm) at a retention time of 7.1 min.

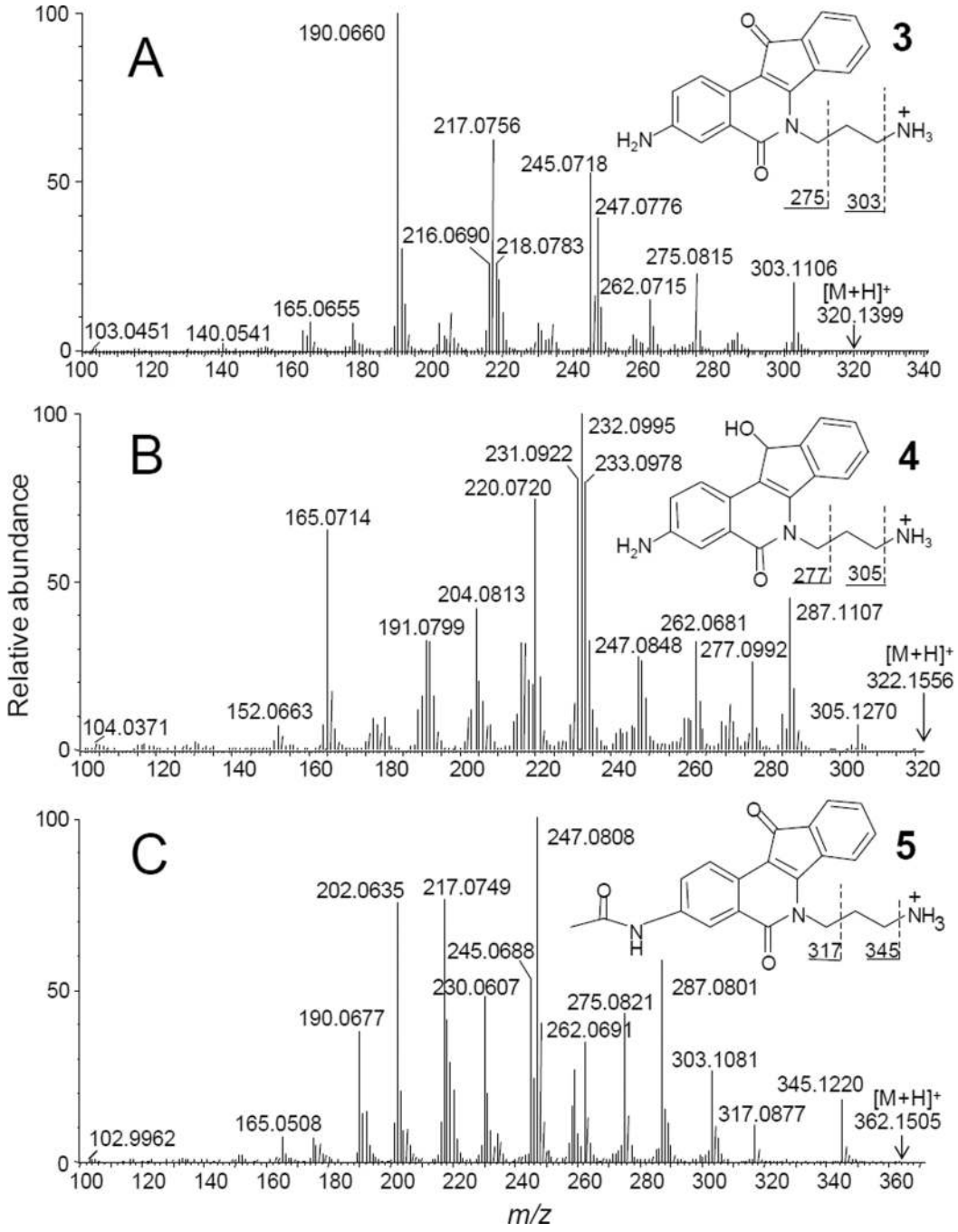

Figure 3.

Positive ion electrospray product ion tandem mass spectra obtained using high resolution accurate mass measurement of A) **3**; B) the abundant phase I metabolite **4**; and C) the abundant phase II metabolite **5**. The mass of the protonated molecule used as the precursor for product ion tandem mass spectrometry is indicated on each tandem mass spectrum.

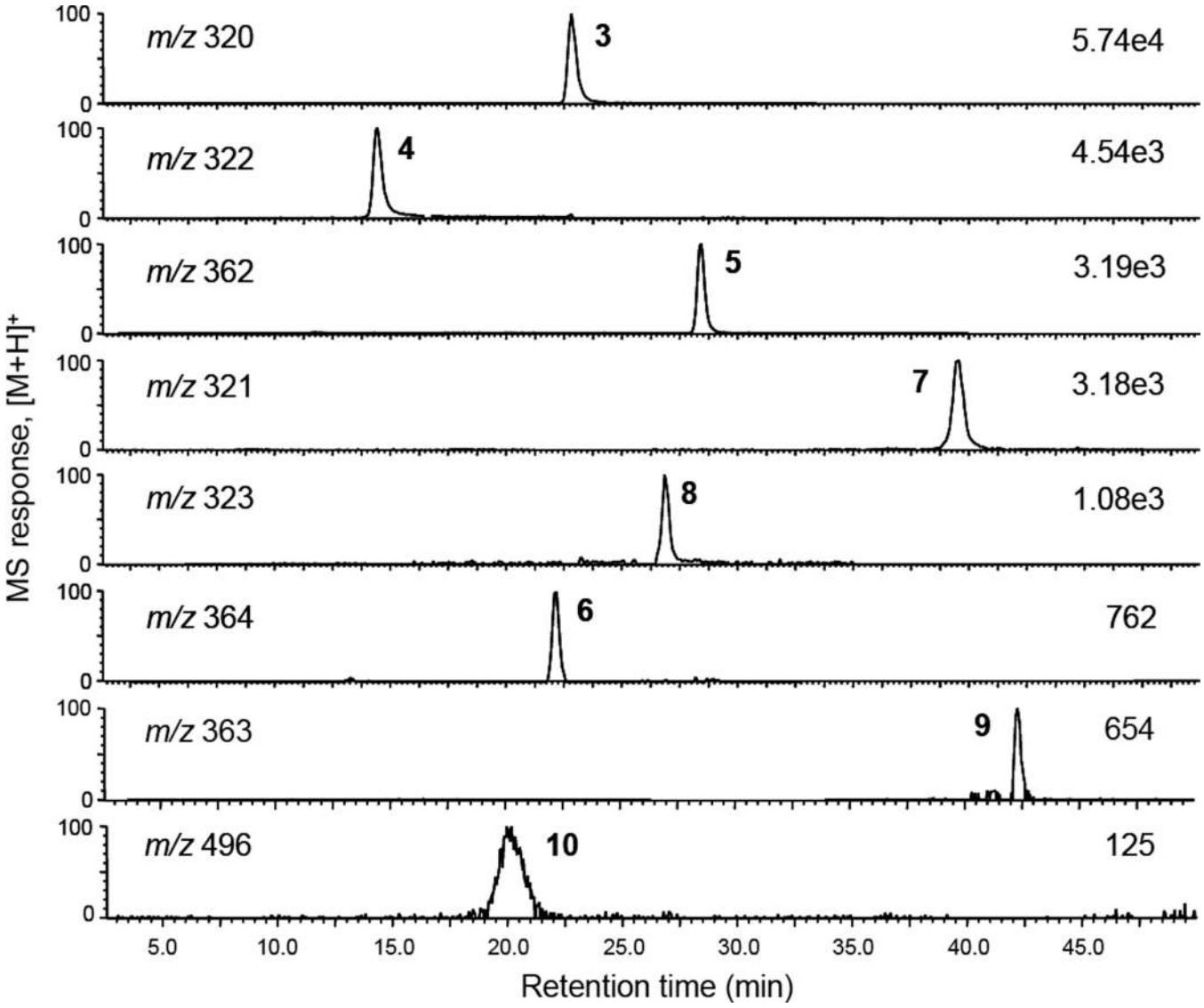

Figure 4.
Computer-reconstructed positive ion electrospray LC-MS chromatograms of **3** and its 7 phase I and phase II metabolites formed during incubation with human hepatocytes.

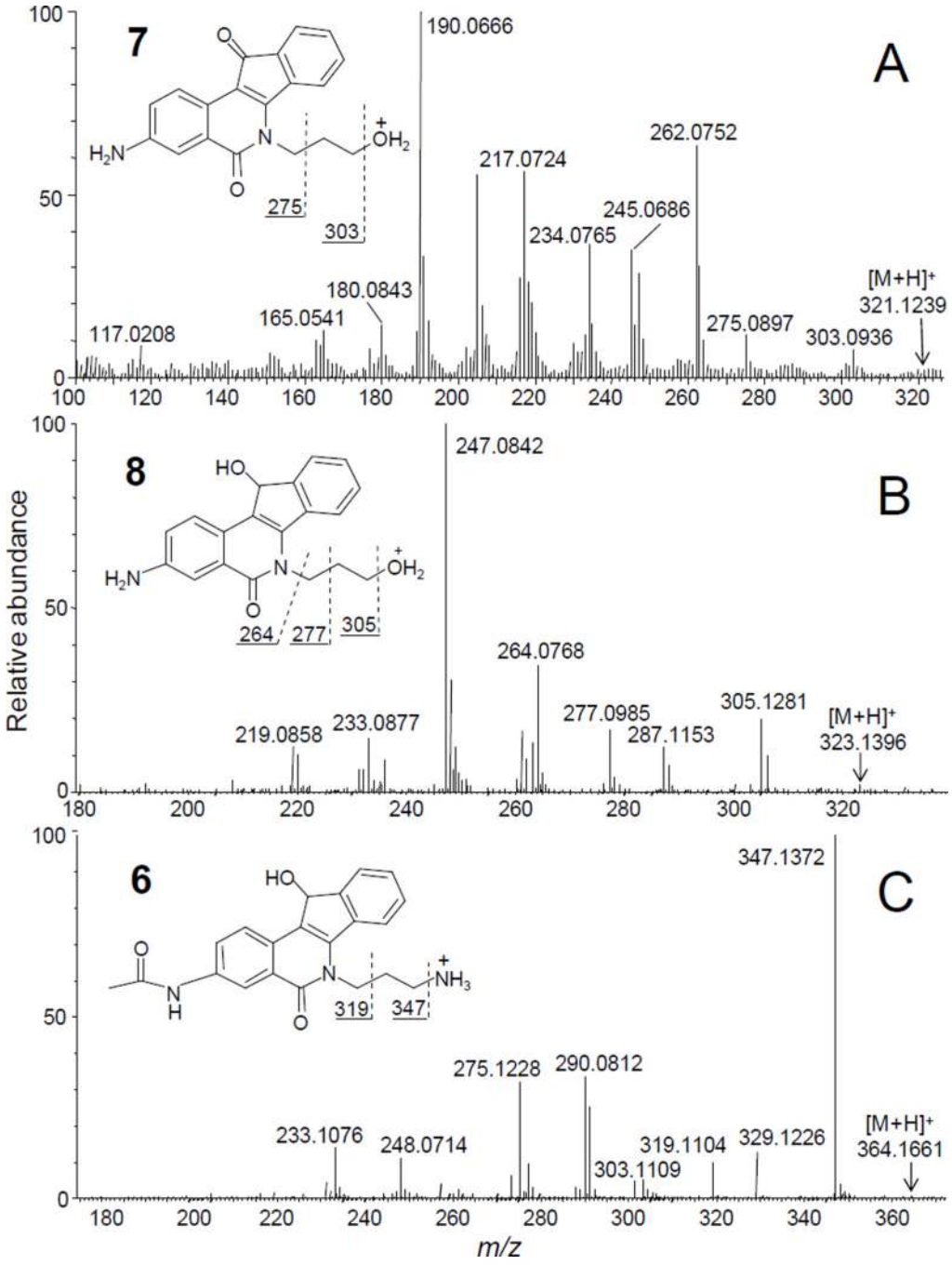

Figure 5.

Positive ion electrospray product ion tandem mass spectra with high resolution accurate mass measurement of A) **7**; B) **8**; and C) **6**. The mass of the protonated molecule used as the precursor for product ion tandem mass spectrometry is indicated on each tandem mass spectrum.

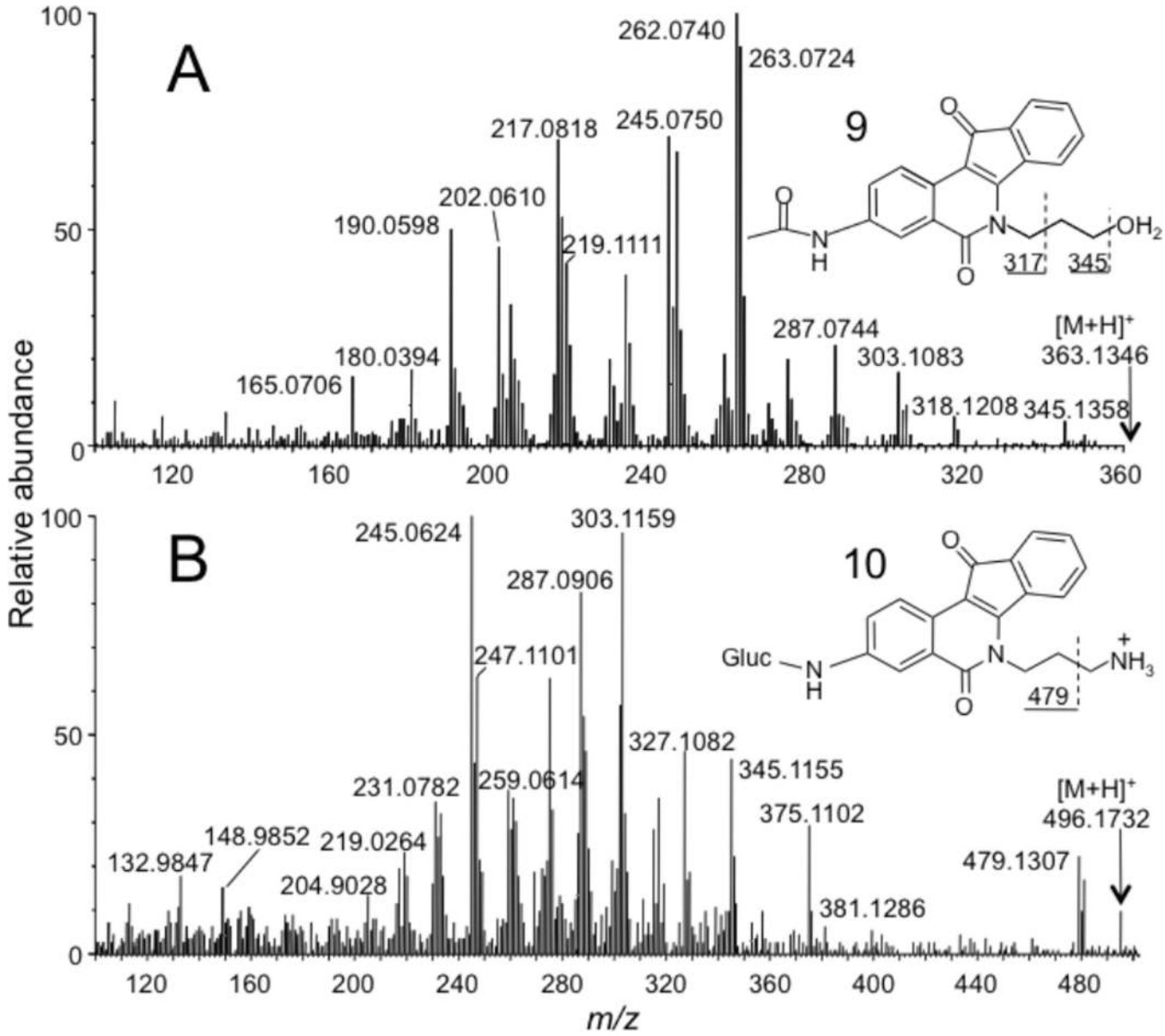

Figure 6.

Positive ion electrospray product ion tandem mass spectra with high resolution accurate mass measurement of A) **9**; and B) **10**. The mass of the protonated molecule used as the precursor for product ion tandem mass spectrometry is indicated on each tandem mass spectrum.

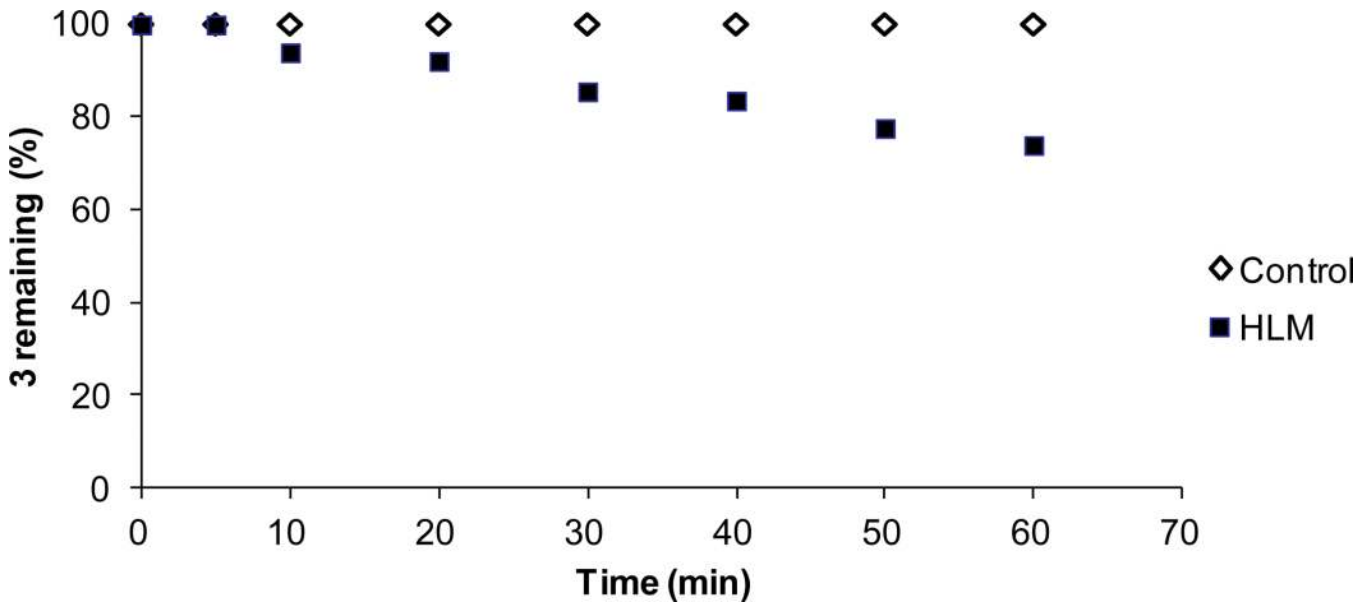

Figure 7.
Disappearance of **3** during incubation with pooled human liver microsomes (HLM).

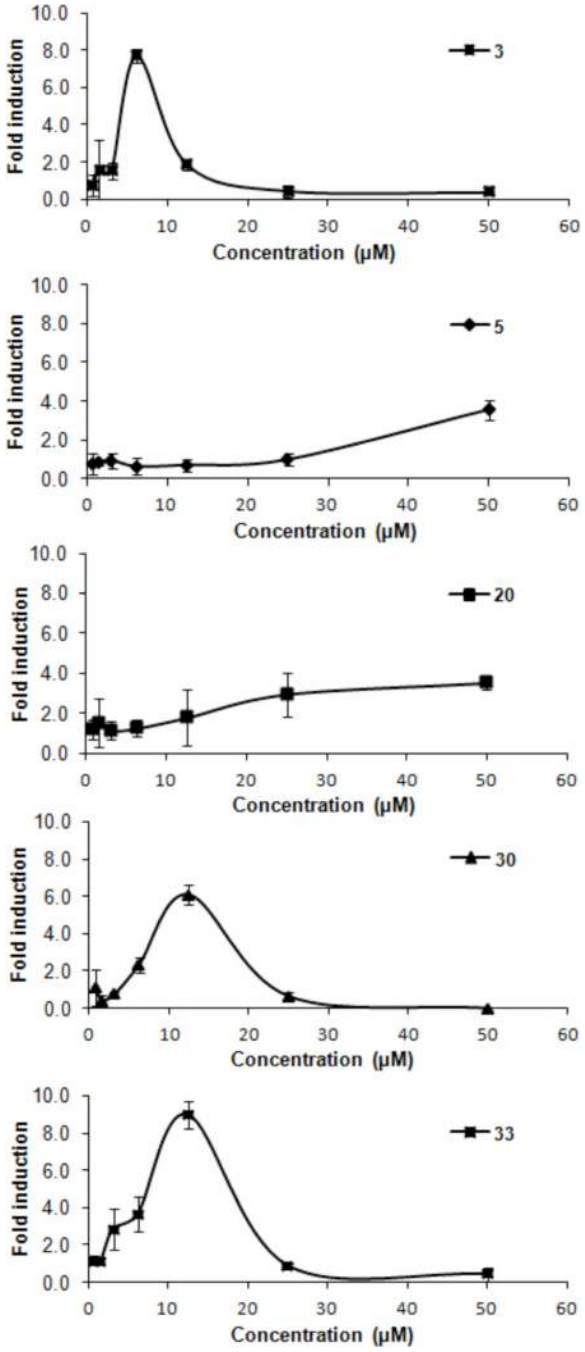

Figure 8.
RXRE induction ratios of active compounds at different concentrations.

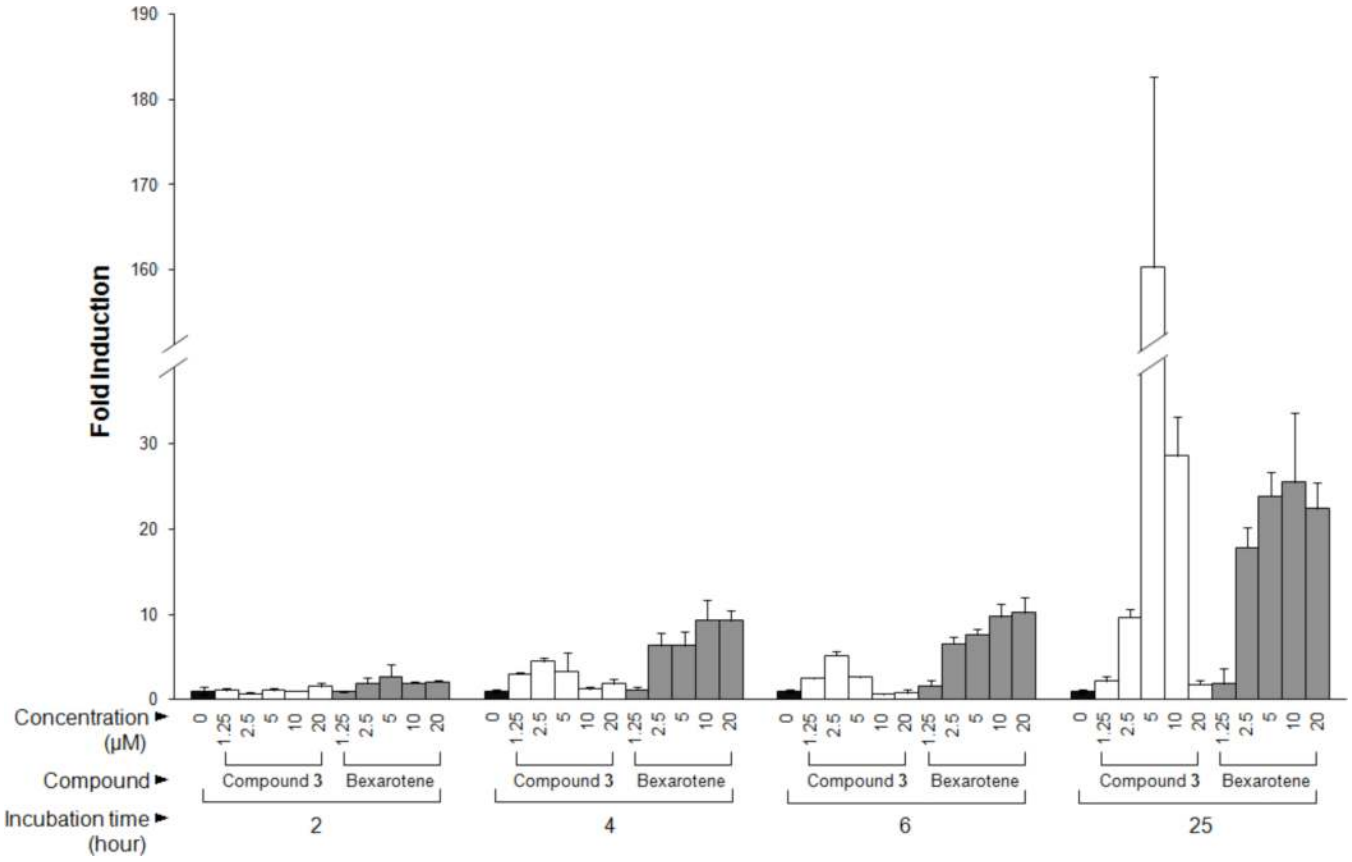

Figure 9.

Comparison of RXRE transcription activity mediated by compound **3** (open bars) and bexarotene (shaded bars) as a function of incubation time and concentration.

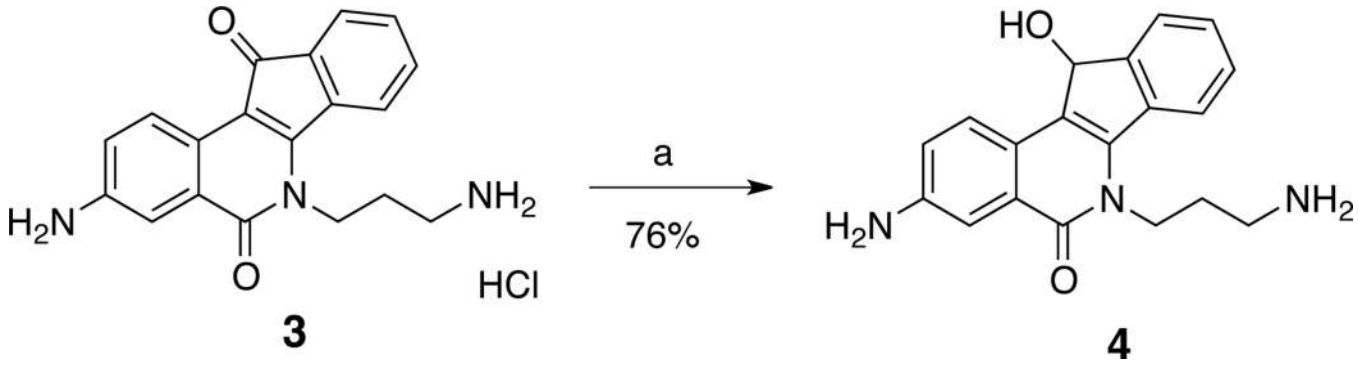

Scheme 1[a]

[a]Reagents and conditions: (a) $NaBH_4$, MeOH, 0 °C.

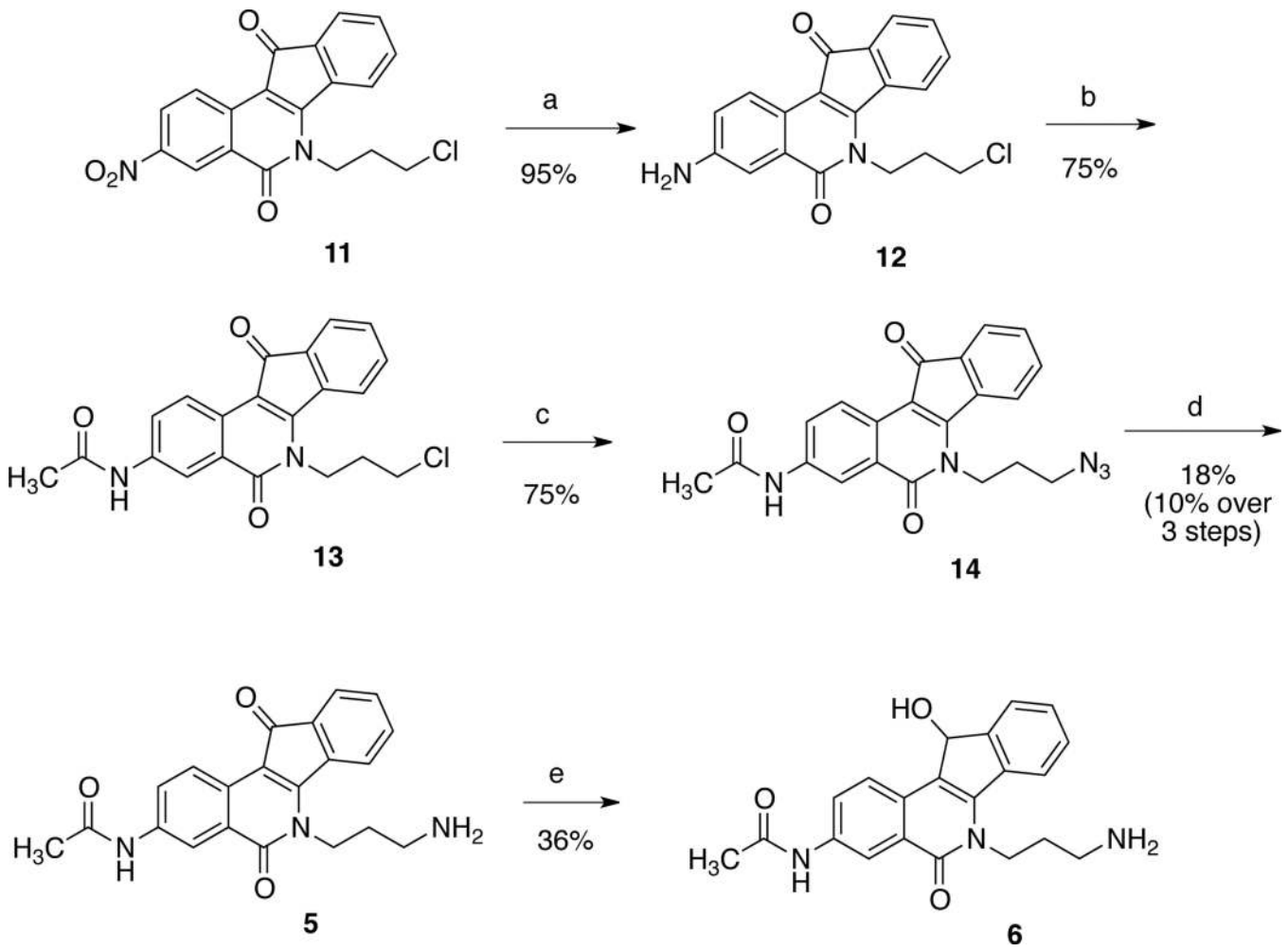

Scheme 2[a]

[a]Reagents and conditions: (a) H_2, Pd-C, MeOH, THF, 50 psi, room temp; (b) AcCl, THF, 0 °C; (c) NaN_3, DMSO, 100 °C; (d) i. $P(OEt)_3$, PhH, reflux; ii. MeOH, HCl, room temp; (e) i. $NaBH_4$, MeOH, 0 °C, ii NH_4Cl, room temp.

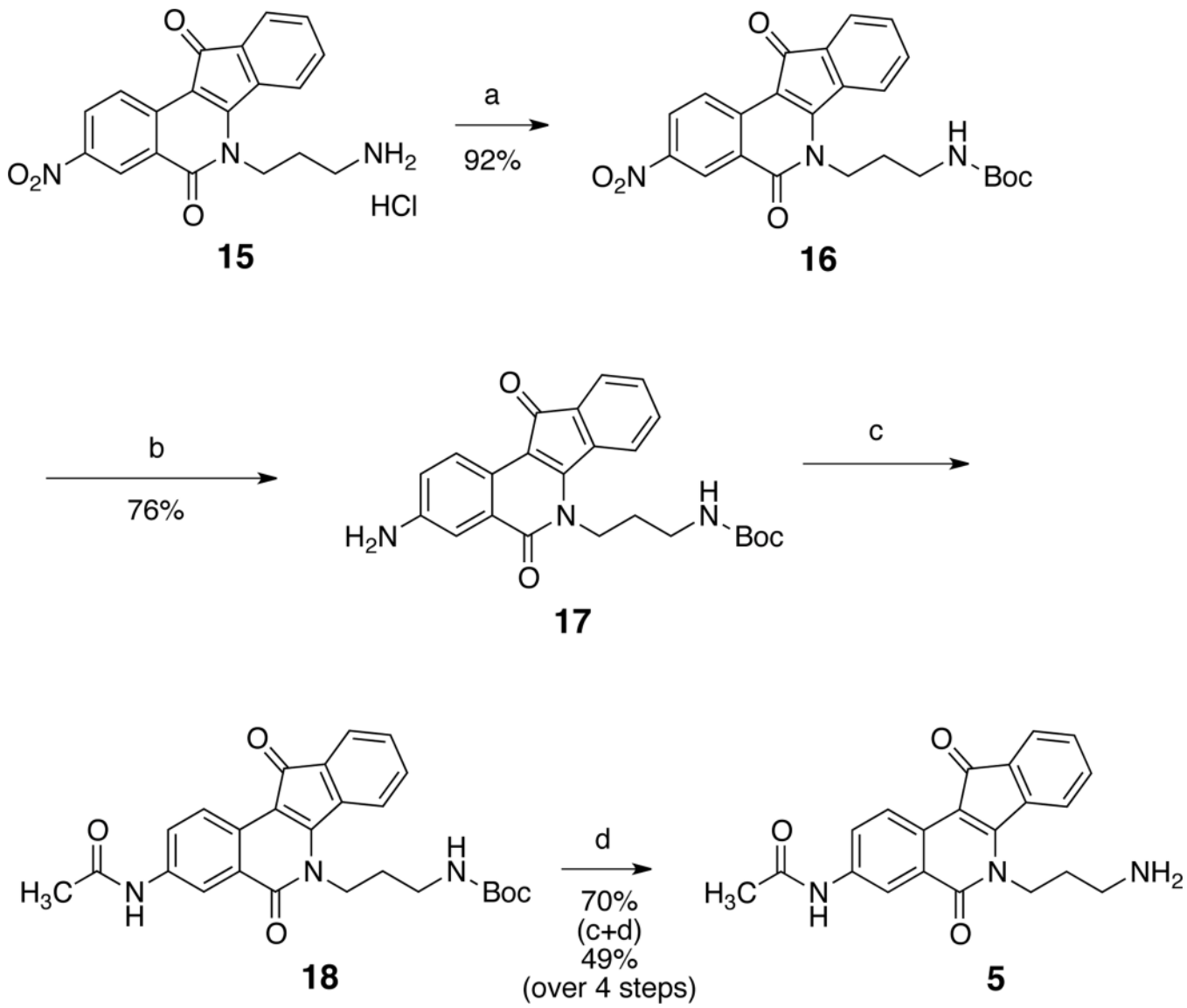

Scheme 3[a]

[a]Reagents and conditions: (a) (tBoc)$_2$O, MeOH, NEt$_3$, 0 °C to room temp; (b) H_2, Pd-C, MeOH, $CHCl_3$, 50 psi, room temp; (c) AcCl, THF, 0 °C to room temp; (d) i. PhH, MeOH, HCl, room temp; ii. K_2CO_3, room temp.

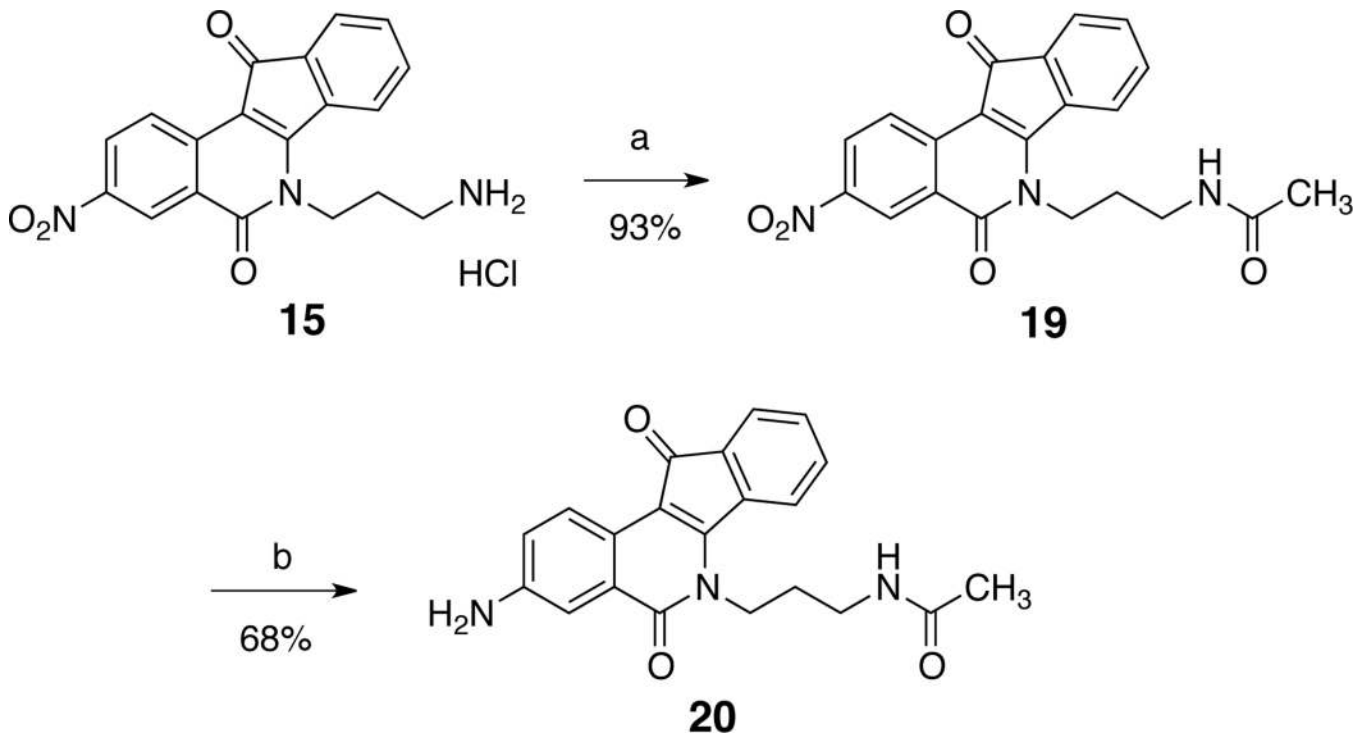

Scheme 4[a]

[a]Reagents and conditions: (a) AcCl, THF, NEt_3, 0 °C to room temp; (b) H_2, Pd-C, DMF, MeOH, THF, 60 psi, room temp.

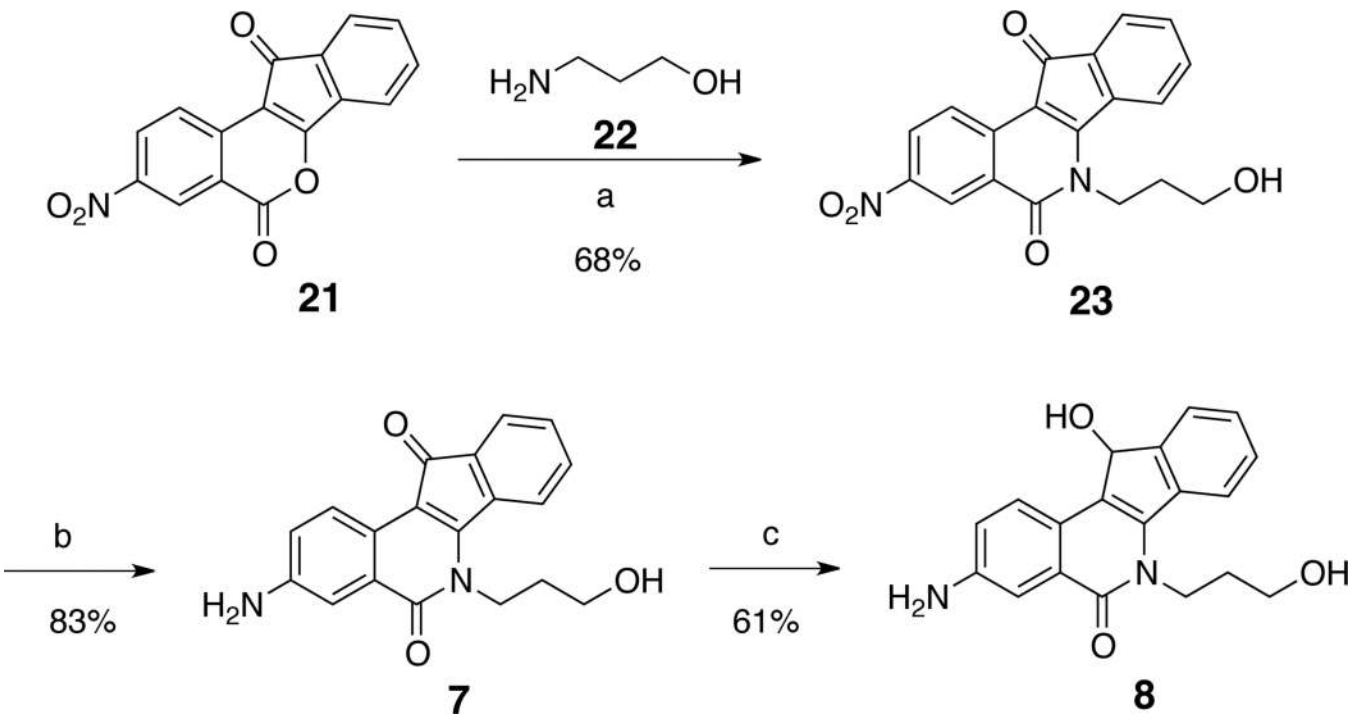

Scheme 5[a]

[a]Reagents and conditions: (a) $CHCl_3$ reflux; (b) i. Fe, NH_4Cl, EtOH, H_2O, reflux; ii. NaOH, reflux; (c) i. $NaBH_4$, MeOH, 0 °C, ii. NH_4Cl.

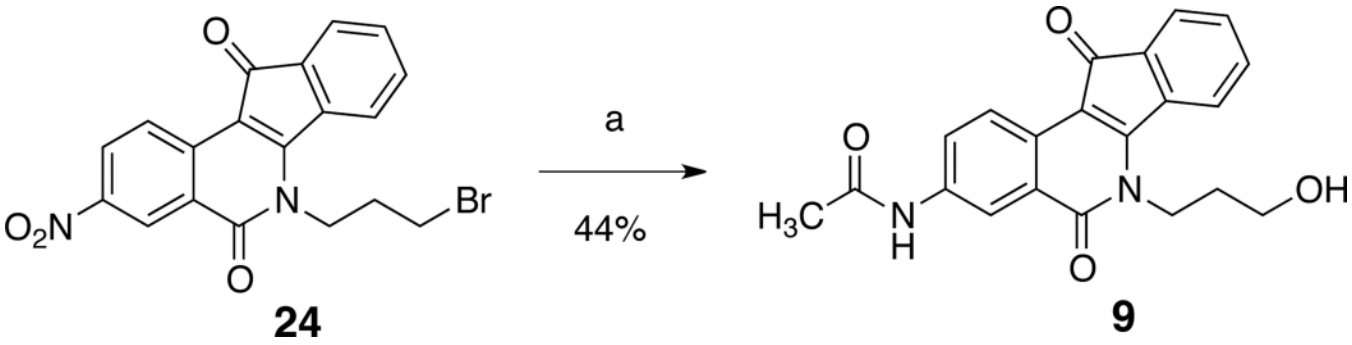

Scheme 6[a]

[a]Reagents and conditions: (a) i. Fe, NH_4Cl,HCl H_2O, EtOH, reflux; ii. NaOH, reflux; iii. AcCl, 0 °C; iv. NaOH, room temp.

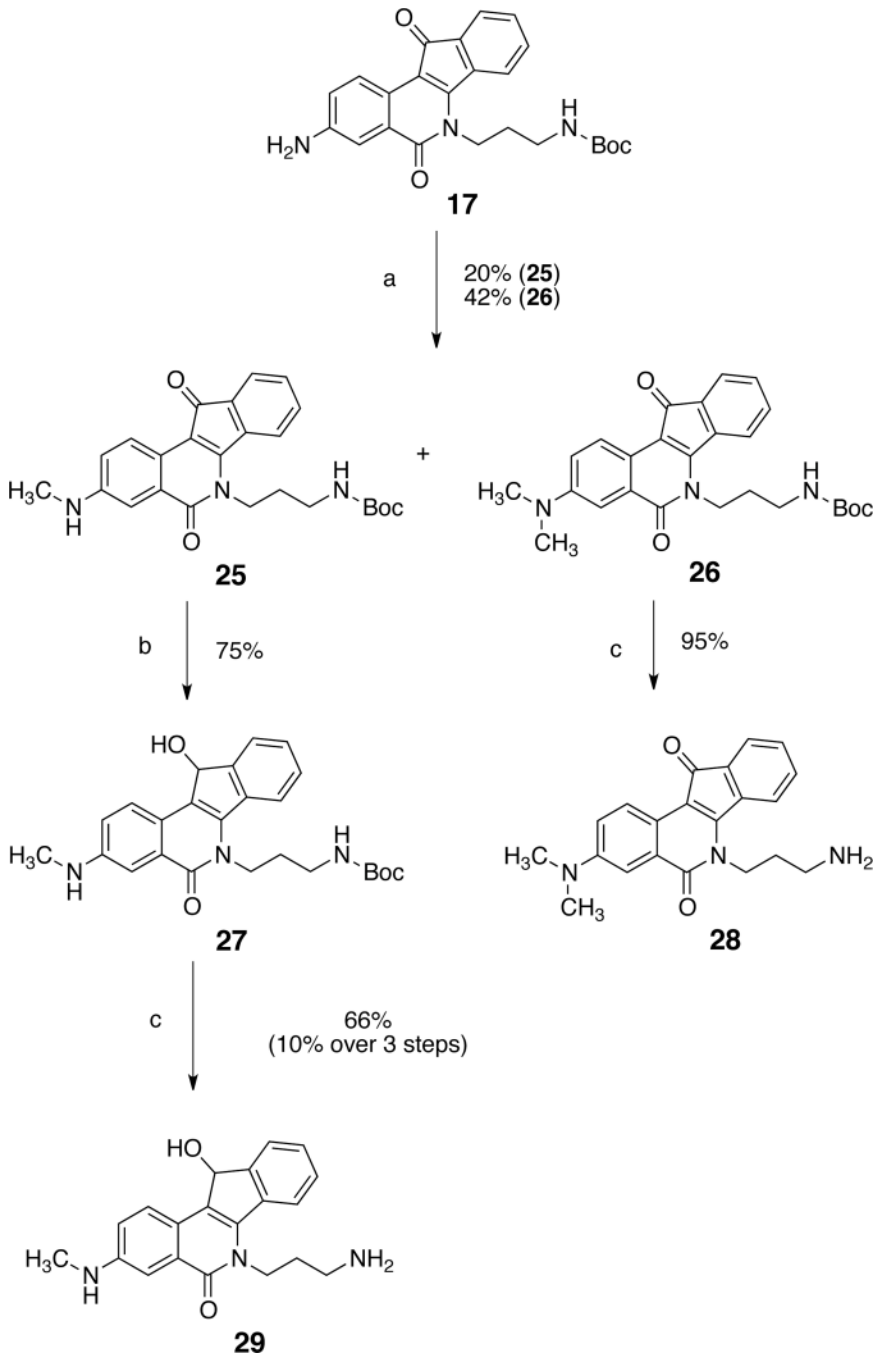

Scheme 7[a]

[a]Reagents and conditions: (a) HCHO, MeOH, AcOH, $NaCNBH_3$, room temp; (b) $NaBH_4$, MeOH, 0 °C; (c) HCl, $CHCl_3$, room temp.

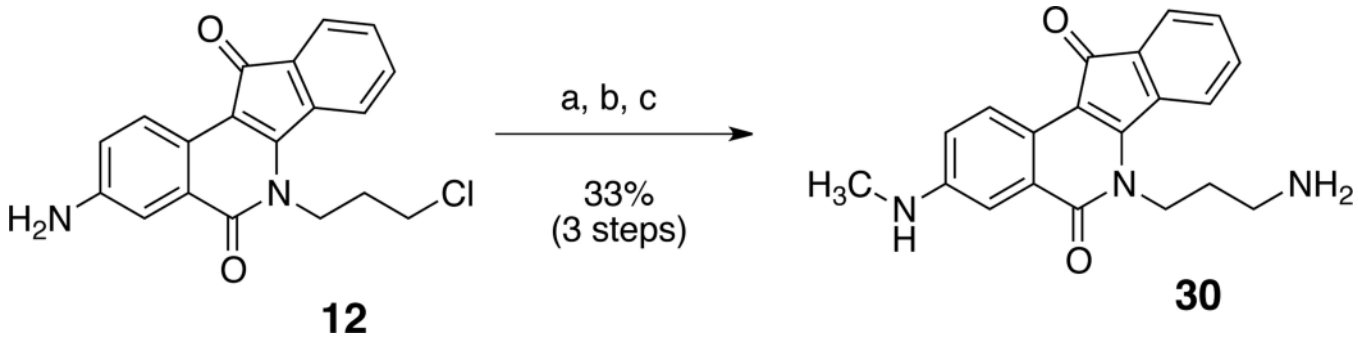

Scheme 8[a]

[a]Reagents and conditions: (a) i. HCHO, MeOH, AcOH, room temp; ii. $NaCNBH_3$, 0 °C to room temp; (b) NaN_3, DMSO, 90 °C; (c) i. $P(OEt)_3$, PhH, reflux; ii. HCl, Et_2O, reflux; iii. K_2CO_3, room temp.

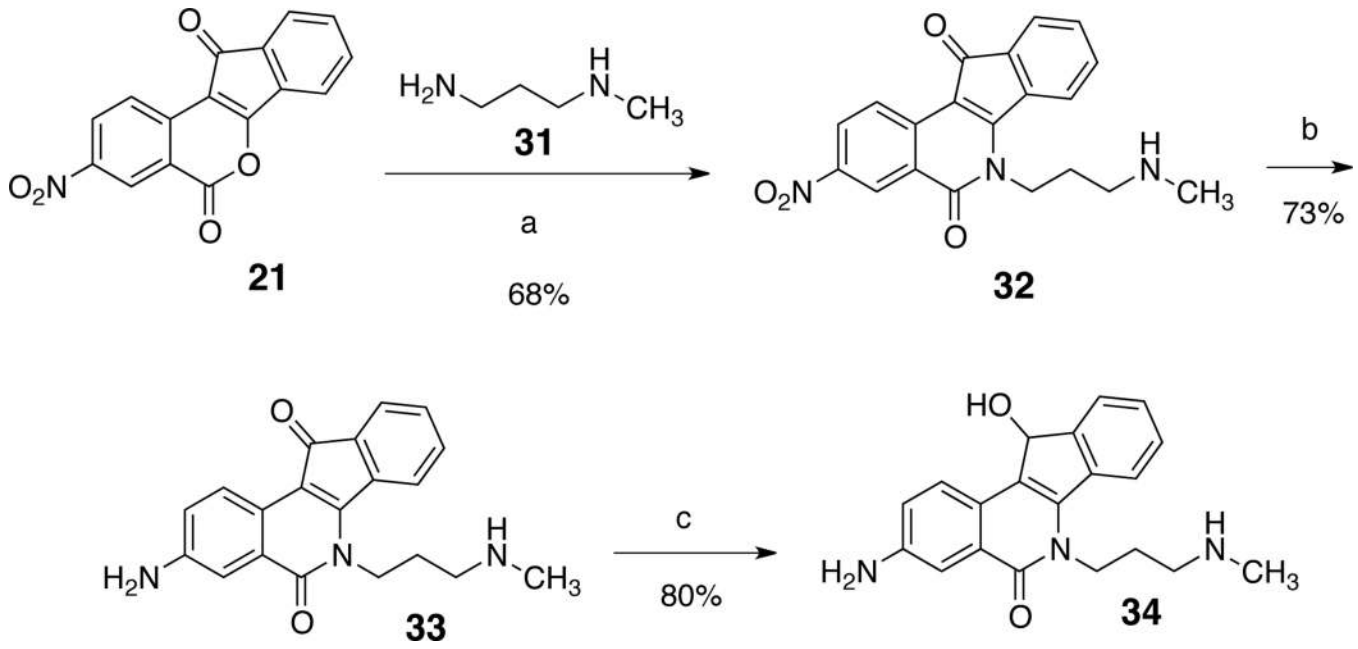

Scheme 9[a]

[a]Reagents and conditions: (a) THF, $CHCl_3$, reflux; (b) Fe, NH_4Cl, EtOH, H_2O, reflux; (c) $NaBH_4$, MeOH, 0 °C.

Table 1

Biological Activities of Bexarotene (**2**), **3**, Metabolites and Synthetic Intermediates

Compd	RXRE				NFκB			
	IR[a,b]	% Cell survival[b]	Highest IR	EC_{50} (μM)[e]	% Inhib.[b]	% Cell survival[b]	IC_{50} (μM)[f]	Cyt IC_{50} (μM)
2	8.85±3.89	74.5±5.1[c]			na[g]	na	na	na
3	0.35±0.10	58.6±0.3	7.67±0.37	3.37±0.51	84.9±3.6	108.7±9.4	26.3±3.0	
4	0.99±0.15	87.5±2.3			53.1±4.5	Cyt[d]		
5	3.55±0.53	74.5±0.6	3.55±0.53	> 41.4	0.0	122.4±6.2		
6	0.97±0.40	83.7±1.3			0.0	99.2±5.9		
7	0.94±0.11	85.9±6.3			53.2	115.6±6.4		
8	0.72±0.11	86.9±2.9			57.8±2.5	118±2.7	49.3±0.6	
9	0.57±0.08	90.6±0.7			53.9±7.8	127.9±10.5		
12	0.99±0.12	102.4±1.6			0.0	91.4±10.4		
14	0.85±0.09	93.1±0.8			0.0	114.6±3.7		
15	0.03±0.07	Cyt			80.8±12	Cyt	2.6±0.4	16.9±1.2
16	0.92±0.16	106.0±2.1			0.0	101.0±1.4		
17	0.60±0.16	104.3±2.6			0.0	107.2±9.7		
19	0.54±0.09	99.4±2.1			87.4±2.5	69.1±12.4	38.8±0.7	
20	3.52±0.33	75.2±1.9	3.52±0.33	20.91±4.47	81.8±2.3	106.3±8.4	14.4±2.8	
23	0.61±0.19	91.4±3.0			72.8±2.5	113.6±1.8	7.3±0.5	
24	0.77±0.08	100.4±0.0[c]			21.8±11	118.5±8		
25	0.85±0.29	94.8±2.6			53.9±1.9	68.6±14.9		
26	0.65±0.50	101.5±1.6			25.9±1.1	97.6±2.6		
27	0.02±0.03	67.5±1.6			83.4±2.3	90.1±11.8	0.4±0.1	
28	0.0	Cyt			86.3±1.6	110.3±2.4	32.3±2.9	
29	0.45±0.26	63.6±2.2			69.2±1.3	95±19.8	0.7±0.1	
30	0.01±0.02	Cyt	6.09±0.51	7.65±1.74	0.0	99.4±10.3		
32	0.00	Cyt			92.4±8.6	79.7±5.2	3.7±0.4	
33	0.44±0.36	64.5±2.6	8.97±0.71	9.96±2.26	63.1±3.2	117±11.2	39.8±2.1	
34	1.31±0.34	84.1±1.5			83.7±0.5	90.1±11.8	0.6±0.1	

[a] IR: induction ratio, or fold induction, at testing concentration;

[b] Testing concentration: 50 μM;

[c] Testing concentration: 40 μM;

[d] Cell survival < 50%;

[e] Concentration required to reach one-half of the maximum IR (see Figure 3);

[f] IC_{50} was calculated when % inhibition >50;

[g] Not available.